LAYER - LATTICE SILICATES:
A SUPPORT FOR A RHODIUM (I) - TRIPHENYLPHOSPHINE HOMOGENEOUS HYDROGENATION CATALYST

Dissertation for the Degree of Ph. D.
MICHIGAN STATE UNIVERSITY
JAMES FRANCIS HOFFMAN
1976

LIBRARY

This is to certify that the

thesis entitled

LAYER-LATTICE SILICATES: A SUPPORT FOR A RHODIUM(I)-
TRIPHENYLPHOSPHINE HOMOGENEOUS HYDROGENATION CATALYST

presented by

James Francis Hoffman

has been accepted towards fulfillment
of the requirements for

Ph.D. degree in Chemistry

T. J. Pinnavaia
Major professor

Date June 14, 1976

O-7639

ABSTRACT

LAYER-LATTICE SILICATES: A SUPPORT FOR A RHODIUM(I)-TRIPHENYLPHOSPHINE HOMOGENEOUS HYDROGENATION CATALYST

By

James Francis Hoffman

The research reported in this thesis demonstrates that smectites, a class of naturally occurring layer-lattice silicate minerals, afford an inorganic and crystalline matrix for supporting cationic homogeneous hydrogenation catalysts. A rhodium(I)-triphenylphosphine complex, $Rh(PPh_3)_x^+$, which is a known hydrogenation catalyst precursor in solution, was introduced into the interlamellar space of hectorite. The rates at which the mineral supported complex catalyzes the hydrogenation of various unsaturated hydrocarbons were measured in methanol under ambient temperature and pressure.

The product of the protonation of $Rh_2(CH_3COO)_4$, $Rh(CH_3COO)_{4-x}^{x+}$ ($x = 1$ or 2), was exchanged onto the surfaces of hectorite. The amount of rhodium exchanged was dependent on the concentration of the green $Rh_2(CH_3COO)_{4-x}^{x+}$ species used in the exchange reaction. For the catalytic studies, a $0.002\underline{M}$ $Rh_2(CH_3COO)_{4-x}^{x+}$ solution was used to prepare the catalyst precursor. The partially exchanged mineral obtained with the $0.002\underline{M}$ solution was found to contain 0.76% Rh, which corresponds to 7.4 mmole Rh/100g of the

mineral. The uv-visible spectrum of a mull of the mineral supported complex exhibits the same intense band that is found for the homogeneous complex at 258 nm. The ir spectrum shows that acetate is coordinated to the rhodium complex.

Upon the addition of triphenylphosphine to the green $Rh_2(CH_3COO)_{4-x}{}^{x+}$-hectorite, an immediate color change to dark orange was observed. This orange mineral bound species, $Rh(PPh_3)_x{}^+$-hectorite exhibited an uv-visible spectrum which contained the same features as $Rh(PPh_3)_3BF_4$ in methanol. The infrared spectrum indicated the presence of triphenylphosphine, and the absence of coordinated acetate in the complex.

Maximum catalytic activity was obtained with the mineral supported catalyst at an initial PPh_3 concentration of 4.6mM. This concentration of PPh_3 corresponded to a PPh_3:Rh ratio of 9:1. For the hydrogenation of 1M 1-hexene, a turnover number of 10.5 ml of H_2/min/mmole of Rh was observed. The mineral environment had an inhibitive effect on the reduction of olefins. A turnover number of 140 ml of H_2/min/mmole of Rh for 1M 1-hexene was observed for the homogeneous catalyst. For terminal olefins, a linear uptake of H_2 was obtained, whereas for substituted olefins, a nonlinear uptake of H_2 was obtained. Internal olefins were not reduced with the mineral supported catalyst. Gas chromatographic analysis of the products of the hydrogenation of 1-heptene showed that some isomerization to 2-heptene occurred during the reaction.

Both internal and terminal alkynes are hydrogenated by the mineral supported catalyst at a rate comparable to the rate with the homogeneous catalyst. 1-Hexyne was reduced at a rate of 530 ml of H_2/min/mmole of Rh, under the same conditions as 1-hexene. Analysis of the products of the reaction by gas chromatography showed that the hydrogenation of 1-hexyne occurred in a stepwise manner, first with the reduction to the olefin, then to the totally saturated hydrocarbon. The reduction of the olefin was insignificant as long as the alkyne concentration was large compared to the olefin concentration. 2-Hexyne was only reduced to the corresponding olefin, at a rate comparable to 1-hexyne.

Similar trends in the relative rates of hydrogenation of both alkenes and alkynes indicated that the catalytic species on the mineral and in solution were chemically similar.

It was not possible to establish the constitution of the catalyst precursor, $Rh(PPh_3)_x^+$, by ^{31}P nmr spectroscopy because of the low solubility of the complex in methanol. However, a dimethylphenylphosphine Rh(I) complex, $Rh(PPh(CH_3)_2)_3BF_4$, was prepared by a reaction of the protonated acetate complex with the phosphine ligand. The nmr study showed that the phosphine acted as the reducing agent in the reduction of $Rh_2(CH_3COO)_{4-x}^{x+}$. Based on the nmr data, PPh_3 was assumed to be the reducing agent in the related $Rh(PPh_3)_x^+$ system.

LAYER-LATTICE SILICATES: A SUPPORT FOR A RHODIUM(I)-TRIPHENYLPHOSPHINE HOMOGENEOUS HYDROGENATION CATALYST

By

James Francis Hoffman

A DISSERTATION

Submitted to
Michigan State University
in partial fulfillment of the requirements
for the degree of

DOCTOR OF PHILOSOPHY

Department of Chemistry

1976

TO LIZ

ACKNOWLEDGEMENTS

I wish to thank Dr. Thomas J. Pinnavaia for the encouragement, advice, and guidance he provided throughout this project. I also wish to express my appreciation to Dr. Carl H. Brubaker, Jr. for serving as my second reader and for all the suggestions on how to improve my writing skills.

No words can express my love and appreciation for Liz, whose love and encouragement made all this possible. She suffered much loneliness, especially during the writing of this dissertation. She was always there with her love during all the happiness and depression one encounters in a project of this magnitude. I also wish to thank my parents, James and Ursula Hoffman, for their continual love and encouragement.

Finally, I wish to thank Michigan State University and the National Science Foundation for their financial support, which made this study possible.

TABLE OF CONTENTS

Page

LIST OF TABLES vi

LIST OF FIGURES vii

I. INTRODUCTION 1

- A. Research Objective 1
- B. Clay Minerals 3
- C. Chemistry of $Rh_2(CH_3COO)_4$ 11
- D. Previous Studies of Supported Homogeneous Catalysts 18

II. EXPERIMENTAL 28

- A. Reagents and Solvents 28
- B. Syntheses 29
  - 1. Methanol Adduct of Tetrakis-μ-acetato-dirhodium(II) 29
  - 2. Protonation of $Rh_2(CH_3COO)_4 \cdot 2CH_3OH$ . . 30
  - 3. Exchanged Hectorites 31
    - a. $Rh_2(CH_3COO)_{4-x}{}^{x+}$-Hectorite 31
    - b. $Rh(PPh_3)_x{}^{+}$-Hectorite 32
- C. Physical Methods 33
  - 1. Gas Chromatography 33
  - 2. X-Ray Diffraction Studies 33
  - 3. UV-Visible Spectra 34
  - 4. Infrared Spectra 34
  - 5. Proton NMR Studies 37
  - 6. Phosphorus-31 NMR Studies 37
- D. Hydrogenation Studies 38

Page

III. RESULTS AND DISCUSSION 44

A. Characterization of the Homogeneous Catalyst 44

1. Solution Chemistry of $Rh_2(CH_3COO)_{4-x}^{x+}$ $(x = 1,2)$ 44

2. Solution Chemistry of $Rh(PPh_3)_3BF_4$ . . 51

B. Characterization of the Heterogeneous Catalyst 65

C. Hydrogenation Studies 72

IV. CONCLUSIONS 92

BIBLIOGRAPHY 93

LIST OF TABLES

Table Page

1. UV-Visible Spectrometric Data 54
2. ^{31}P and ^{19}F NMR Data 61
3. Rhodium Loading on Hectorite 65
4. Hydrogenation Rates of Alkenes in the Presence of Mineral Supported and Homogeneous Rh(I)-PPh_3 Catalysts 77
5. Hydrogenation Rates of Alkynes in the Presence of Mineral Supported and Homogeneous Rh(I)-PPh_3 Catalysts 85
6. Effect of Rhodium Loading on the Turnover Number 91

LIST OF FIGURES

Figure Page

1. (a) Octahedral-Tetrahedral Array of Smectites (b) Hexagonal Network of the Tetrahedral Layer 5
2. Layer Structure of Smectites Illustrating the Intracrystalline Space Which Contains the Exchangable Cations 8
3. Infrared Spectra of Na^+-Hectorite; (a) After Treatment with Sodium Bisulfate to Remove Calcium Carbonate Impurity, (b) Before Treatment with Sodium Bisulfate 36
4. Schematic of Hydrogenation Apparatus 40
5. Reaction Flask with Adaptors for Connecting to the Hydrogenation Apparatus 42
6. Possible Products of the Protonation of Rhodium(II) Acetate; (a) Rhodium(II) Acetate, (b) *Tris*(acetato)dirhodium(II), (c) *Trans-bis*(acetato)dirhodium(II), (d) *Cis*-*bis*-(acetato)dirhodium(II) 47
7. ^1H NMR Spectrum of the Products of the Protonation of Rhodium(II) Acetate Performed in a Sealed NMR Tube 49
8. Visible Spectra Which Show the Progress of the Protonation of Rhodium(II) Acetate; (1) After 14 Hours, (2) After 23 Hours, (3) After 41 Hours, (4) After 112 Hours . . 53

Figure Page

9. ^{1}H NMR Spectra of (a) Products of the Protonation of Rhodium(II) Acetate, (b) The Same Solution After the Addition of Triphenylphosphine 56
10. ^{31}P NMR Spectrum of $Rh(PPh(CH_3)_2)_3BF_4$ in Methanol 60
11. Solution Sturucture of $Rh(PPh(CH_3)_2)_3BF_4$ . . 62
12. UV-Visible Spectrum of $Rh(PPh_3)_3BF_4$ in Methanol 64
13. Infrared Spectra of Various Hectorites; (a) Sodium(I)-Hectorite After Treatment with Sodium Bisulfate, (b) The Same Mineral After Washing with Methanol, (c) $Rh_2(CH_3COO)_{4-x}{}^{x+}$-Hectorite, (d) $Rh(PPh_3)_x{}^+$- Hectorite 68
14. UV-Visible Spectrum of $Rh(PPh_3)_x{}^+$-Hectorite. 71
15. Adsorption Curve of Triphenylphosphine on Na^+-Hectorite 75
16. Plot of the Hydrogenation Rate of 1-Hexene . 80
17. Plot of the Hydrogenation Rate of Allyl Alcohol 83
18. Plot of the Hydrogenation Rate of 1-Hexyne . 87
19. Plot of the Hydrogenation Rate of Propargyl Alcohol 90

I. INTRODUCTION

A. Research Objective

In recent years, there have been many reports which have dealt with the attachment of homogeneous catalysts to insoluble matrices as a means of combining most of the advantages of homogeneous and heterogeneous catalysis.

The advantages of homogeneous catalysis over heterogeneous catalysis are:[1]

1. The catalysts usually exhibit higher selectivity.
2. The reactions are mechanistically easier to study, and occur under less stringent conditions.
3. All catalytic sites are accessible, therefore less catalyst is generally required.
4. The properties of the catalyst can be varied by changing the ligands; eg., the use of a chiral ligand may lead to the formation of optically active products from prochiral substrates.

The main disadvantages of homogeneous catalysis are the difficulty of removing the products from the reaction mixture without loss of activity, and the ease at which the catalyst can be poisoned. With the exception of the Oxo-process, industrial processes employ heterogeneous catalysts because it is generally not economically feasible to separate the homogeneous catalyst from the products in solution.

Supported homogeneous catalysts, besides combining the advantages of homogeneous and heterogeneous catalysis, give rise to several other characteristics unique to these systems. The supported catalysts often lead to reaction selectivity based on size or polarity of the substrate. The selectivity is similiar to the effect that the surrounding protein exerts on the active site in an enzyme. Certain complexes, which are not catalytically active in solution because they undergo dimerization, may be activated when attached to a support which is sufficiently rigid to prevent the recombination of the monomeric units.

There exists a class of layer-lattice silicate minerals generally known as smectites or "swelling clays", which are capable of bonding transition metal ions and organometallic cations in their interlamellar space. These minerals are structurely unique, and represent novel crystalline inorganic matrices for supports of homogeneous catalysts. Smecties are ubiquitous, relatively inexpensive, and usable as supports without pretreatment. The principal factor in the selection of a catalyst which is to be supported in the mineral environment, is that the homogeneous complex must be cationic.

The objective of this research project was to investigate the chemistry of a known homogeneous hydrogenation catalyst in solution and on the surfaces of the mineral. The hydrogenation reaction was chosen for study because the basic chemistry of this reaction is well investigated and there exist many known cationic transition metal complexes which function as homogeneous hydrogenation catalysts.[2] The complex selected for study was a Rh(III) hydride derived from $Rh_2(CH_3COO)_4$ according to the method of Wilkinson and coworkers.[3]

The two questions of main interest at the start of this thesis research were:

1. Will a homogeneous catalyst, when exchanged onto the silicate surfaces, retain its chemical constitution and catalytic activity?
2. Does the environment of the mineral modify the selectivity of the catalyst relative to its selectivity in solution?

B. Clay Minerals

The term "clay", as used in geology and soil science, refers to any inorganic material with a particle size $<2\mu$.[4] However, the term "clay", as used in this thesis, refers to the layer-lattice silicate minerals hectorite and montmorillonite.

These minerals are composed of silicon, aluminum, oxygen, iron, alkali and alkaline earth cations. They are capable of adsorbing large amounts of water and a variety of other molecules. The adsorption process can occur in the region between the crystalline sheets and can cause one crystallographic dimension to increase dramatically. These minerals are structurally similar to talc and pyrophyllite.

The talc and pyrophyllite structures consist of two tetrahedral arrays of silica which sandwich an octahedral array of alumina as in pyrophyllite or of magnesia as in talc. These aluminosilicate sheets are stacked to form crystallites. The schematic in Figure 1a depicts the three-layer arrangement of the tetrahedral and octahedral holes in

Figure 1. (a) Octahedral-Tetrahedral Array of Smectites
(b) Hexagonal Network of the Tetrahedral Layer

(Adapted from reference 4)

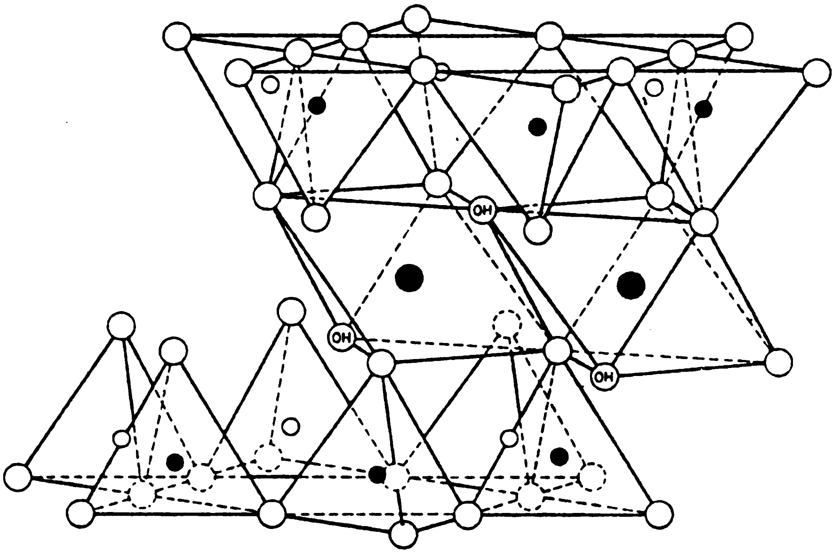

(a)

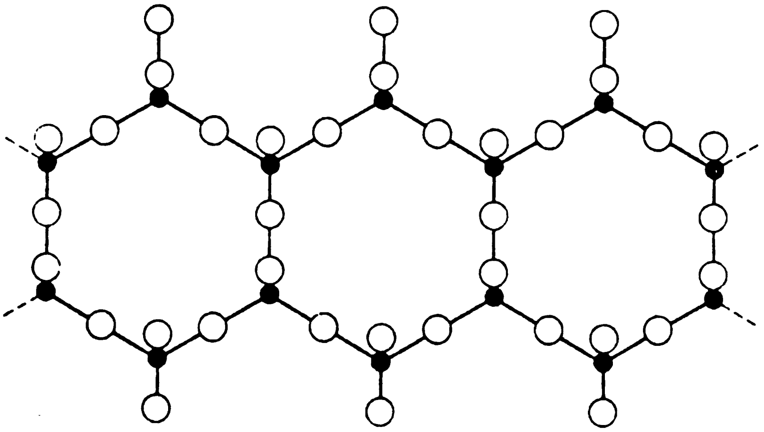

(b)

the silicate sheets. The idealized structure has a silicon atom in the center of each tetrahedron and all the tips of the tetrahedra point toward the central octahedral layer. The base of the tetrahedrons are arranged to form an infinite hexagonal network (cf., Figure 1b). The octahedral layer is formed from shared oxygen atoms of the tetrahedral layers and an occasional hydroxyl group, which is needed to balance the charge. The thickness of the three-layer sheet is 9.6Å. When all the tetrahedral holes are filled with silicon atoms and all the octahedral holes are filled with magnesium atoms, the neutral unit, $(Mg_6)[Si_8]O_{20}(OH)_4$, represents the unit cell formula of talc, a trioctahedral mineral. If only two-thirds of the octahedral positions are occupied by aluminum atoms, the neutral dioctahedral unit pyrophyllite, $(Al_4)[Si_8]O_{20}(OH)_4$, is obtained. These minerals are held together by van der Waals forces, which give rise to the characteristic flakes of these minerals. Since these flakes are relatively large, greater than 2μ, these minerals are classified as micas.

Pyrophyllite and talc represent the parent members of the three-layer smectite minerals. The smectites differ from the micas by substitutions within the tetrahedral and octahedral layers. Cations of similar size but of lower charge are substituted into the aluminosilicate layers, which give rise to a net negative charge within these layers. This charge is balanced by cations of variable solvation which are located in the region between the anionic sheets (cf., Figure 2). In the naturally occurring minerals, these

Figure 2. Layer Structure of Smectites Illustrating the Intracrystalline Space Which Contains the Exchangable Cations

(Adapted from reference 4)

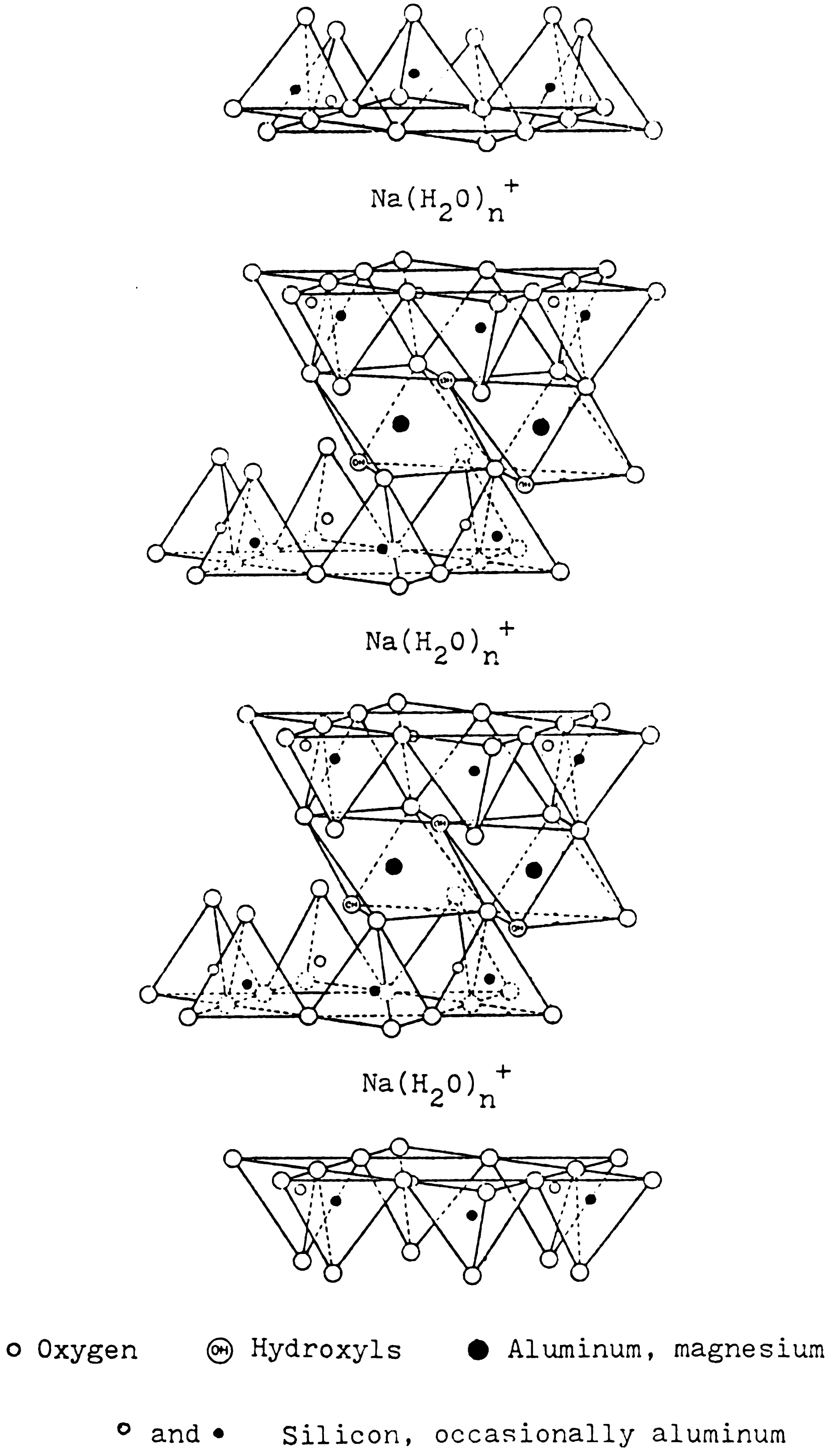
$Na(H_2O)_n^+$
$Na(H_2O)_n^+$
$Na(H_2O)_n^+$
○ Oxygen
⊛ Hydroxyls
● Aluminum, magnesium
° and • Silicon, occasionally aluminum

interlayer ions are either sodium (Na^+) or calcium (Ca^{2+}). They can easily be replaced by transition metal cations or organic cations, which can dramaticly change the swelling and adsorption properties of the mineral.

Several factors have been pointed out by van Olphen[5] to have an effect on swelling: the solvation energy of the cations, the energy of adsorption of the solvent onto the surfaces, and the electrostatic energy between the charged species. Solvent polarity plays a role in determining whether cation solvation energy or surface solvation is the predominate force.

The structure of hectorite is derived from that of talc. By an isomorphous substitution of Li^+ for some Mg^{2+} in the octahedral positions, the idealized unit cell formula of hectorite, $Na_{0.66}(Mg_{5.34}Li_{0.66})[Si_8]O_{20}(OH)_4$, is obtained. Montmorillonite has a similar substituion in the octahedral layer where Mg^{2+} replaces some Al^{3+} ions. The idealized unit cell formula of a typical montmorillonite is $Na_{0.66}(Al_{3.34}Mg_{0.66})[Si_8]O_{20}(OH)_4$. Both of these minerals are capable of swelling to a large extent in the presence of water. Iron and other trace metals which occupy tetrahedral or octahedral sites in the silicate sheets are omitted from the idealized formulas.

Vermiculite, a mineral related to the smectite class, has a larger negative charge in the silicate sheets. In contrast to hectorite and montmorillonite, the charge deficiency arises from the isomorphous substitution of Al^{3+} for some Si^{4+} in the tetrahedral layers. The result of these changes is vermiculites have a reduced swelling capability. Under optimum hydration conditions, the mineral will swell to allow two monolayers of water in the intracrystalline space, whereas hectorite and montmorillonite will swell to accommodate multiple monolayers of water. In a water slurry, hectorite and montmorillonite will swell to approximately 100Å so that under these conditions the sheets are totally separated. For each monolayer water adsorbed in the interlayer, the basal spacing (001) increases by approximately 2.5Å. This interlayer thickness remains constant at intergrals of 2.5Å over a large range of partial pressures of water, then increases abruptly. This stepwise change in interlayer thickness with increasing water uptake indicates that the intercrystalline water is well structured before the monolayer is complete.

In addition to the interlamellar cations, exchangeable cations are located on edge sites, which arise from bond breakage along the edges of the mineral. Hydroxyl groups are attached to the silicons of the broken tetrahedral units to form Si-OH groups. These Si-OH groups are ionized similarly to silicic acid:

$$\text{Si-OH} + \text{OH}^- = \text{Si-O}^- + \text{H}_2\text{O} \qquad (1)$$

which causes a negative charge on the lattice at high pH. The negative charge decreases as the pH is lowered. The edge sites can account for approximately 20% of the total cation exchange capacity (CEC) when the particle size is <2μ.

Clay minerals have been employed as catalysts for many years. They were used by the petroleum industry as some of the first cracking catalysts. The cracking reactions were catalyzed by Lewis and Bronsted acid sites on the surfaces of the minerals. The early work in clay mineral catalysis has been reviewed by Grandquist.[6]

Recently, the clay minerals have been used as catalysts for other types of reactions. Fenn, et al.[7] have reported the dimerization of anisole to 4,4'-dimethoxybiphenyl on Cu^{2+}-hectorite over P_2O_5. The formation of porphyrins and porphyrin intermediates on various transition metal ion montmorillonites has recently been reported.[8] Also, Welty and Pinnavaia[9] have reported the hydrogenation of 1-hexene by using a rhodium exchanged hectorite. In all these cases, the catalytic reaction occurred in the interlamellar space of the mineral, and the metal ion was involed in the catalytic process.

C. The Chemistry of $Rh_2(CH_3COO)_4$

Although there exists a vast quantity of published research on Co^{2+} (d^7) chemistry, there is comparably little work published on its congener, Rh^{2+}. Prior to 1962, no complexes of Rh(II) were known, but Rh(II) was postulated to exist as an intermediate in reactions of Rh(III). Chernyaev, et al.[10] were the first to synthesize a Rh(II) species, $Rh_2(CH_3COO)_4 \cdot 2H_2O$. This complex was investigated by X-ray crystallography[11] and was found to be isostructural to copper(II) acetate and chromium(II) acetate. These complexes contain a metal-metal bond and four bridging acetate ligands.

The sixth coordination site is occupied by a solvent molecule, which can readily be displaced by another donor molecule. The sixth coordination position can also be vacant by removing the solvent molecule with vacuum and heat treatment. The earliest work in Rh(II) chemistry consisted of studying the properties of the different adducts of rhodium(II) acetate.[12]

The acetate ligands can be replaced by a variety of related carboxylate ligands, eg., CF_3COO^-, CCl_3COO^-, and $C_6H_5COO^-$, simply by allowing $Rh_2(CH_3COO)_4$ to react with an excess of the requisite carboxylic acid. By this method, Cotton, et al.[13] were able to prepare $Rh_2(C_6H_5COO)_4$ which previously was only able to be prepared as a triphenylphosphine adduct, $Rh_2(C_6H_5COO)_4 \cdot 2PPh_3$.[3] A kinetics study of the exchange reaction between various carboxylate ligands and acetate showed that the first acetate bridge was difficult to remove, but once the first ligand was replaced, the second bridge was removed easily. The remaining two ligands were more difficult to remove than the first.[14]

Rhodium(II) acetate is an active catalyst for the hydrogenation of terminal olefins in a variety of polar organic solvents.[15,16] This complex also catalyzes the hydrogenation of alkynes, but the rate of reduction is slower than for olefins. The catalytic reaction is known to occur at only one rhodium atom, and involves the heterolytic splitting of hydrogen to form a monohydride. This hydride then reacts with the olefin. The catalyst is not poisoned by oxygen, instead it reduces O_2 to water.

Interest in Rh(II) increased when Maspero and Taube[17] reported the simple dimeric complex, $Rh_2(H_2O)_{10}^{4+}$, in which bridging ligands were absent. They were able to reduce Rh(III) with Cr^{2+} by an inner sphere one electron transfer:

$$2Rh(H_2O)_5Cl^{2+} + 2Cr^{2+} = Rh_2(H_2O)_{10}^{4+} + 2CrCl^{2+} \quad (2)$$

This aquo complex was stable under nitrogen at room temperature. Ion exchange chromatography and conductometric titration studies verified the presence of a +4 charge. No anion was found to precipitate the complex, and a salt has not been isolated.

Ziolkowski and Taube[18] have pointed out that Rh_2^{4+} in dilute solution was obtained by the reduction of $RhCl^{2+}$ with Cr^{2+} as long as the starting solution has a $Cl^-:Rh \leq 1$; otherwise rhodium metal was formed. Also, Rh_2^{4+} is obtained without formation of rhodium metal in a reaction between $Rh(NH_3)_5Cl^{2+}$ and Cr^{2+} in the presence of EDTA. The electron transfer reaction proceeded by an inner-sphere mechanism through a Cl^- of H_2O bridge. After the transfer of an electron, the $Rh(H_2O)_5^{2+}$ moiety then dimerized to form $Rh_2^{4+}{}_{(aq)}$.

The oxidation of Rh_2^{4+} to Rh(III) was discussed by Ziolkowski.[19] In the presence of dioxygen, a violet product, $[Rh_2(H_2O)_{10}O_2]^{4+}$, was obtained. The author suggested that this complex contains a peroxo bridge between the rhodium atoms. When Rh_2^{4+} was allowed to react with NO, a monomeric complex, $[Rh(H_2O)_5NO]^{2+}$ was formed.

Rhodium(II) acetate, which is a d^7 complex with a metal-metal bond, is expected to be diamagnetic. However,

$Rh_2^{4+}{}_{(aq)}$ was found by Maspero and Taube[17] to be slightly paramagnetic. The paramagnetism was attributed to an equilibrium between the dimer and the monomer:

$$Rh_2^{4+} = 2Rh^{2+} \qquad (3)$$

The paramagnetism could be explained by 6-10% deviation of the dimer. Belova and Dergacheva[20] have measured the magnetic susceptibility of anhydrous rhodium(II) acetate and other acetato complexes of Rh(II). They found the susceptibility to be constant, $\mu_{eff} = 0.52 \pm 0.05$ BM, over the temperature range studied. It was concluded that the slight paramagentism was due to temperature-independant paramagnetism (TIP). This form of paramagnetism arises from coupling of the ground state with excited states of the complex when the complex is placed in a magnetic field. Taube has retracted his interpretation of the susceptibility of Rh_2^{4+}, and now attributes the observed paramagnetism to TIP, not the equilibrium between the dimer and the monomer.[21]

Legzdins, _et al_.[3,22] reported the synthesis of Rh_2^{4+} prepared in methanol by the protonation of $Rh_2(CH_3COO)_4$ with a strong non-complexing acid, _eg_., HBF_4 or CF_3SO_3H.

$$Rh_2(CH_3COO)_4 \xrightarrow[CH_3OH]{H^+} Rh_2^{4+} + CH_3COOH + CH_3COOCH_3 \qquad (4)$$

They also were unable to isolate a stable salt. The protonated species was reported to be stable in air. The complex was characterized by uv-visible spectroscopy and by the analysis of the uncoordinated acetate, as acetic acid and methyl acetate, which indicated that all four acetates were removed by the protonation. The electronic spectrum was similar, but not identical, to the spectrum of $Rh_2^{4+}(aq)$ reported by Maspero and Taube.[17] The protonated species could be reconverted to $Rh_2(CH_3COO)_4$ by the addition of excess sodium acetate. More recently, Wilson and Taube[23] have reported that depending on the length of treatment, only one or two acetate ligands were removed by protonation. They were unable to reproduce the results of Legzdins, _et_ _al_.[3,22] This discrepancy will be discussed in greater detail later in this thesis.

The electronic spectra of all the dimeric Rh(II) species are remarkably similar; they all exhibit two bands in the visible region, a low energy band in the range of 590-650 nm, and a higher energy band between 400-450 nm. Two groups have studied the effects of different ligands on the visible absorption spectrum.[24,25] Each group has derived a different MO diagram, but their basic conclusions are similar. The high energy band (band II) is insensitive to changes in the axial ligands, whereas the low energy band (band I) is sensitive to changes in the axial ligands. The pronounced sensitivity of band I to changes in the axial ligands indicates that the transition involves the d_{z^2} orbital on rhodium. Most likely this orbital is the one in which the transition terminates. Band II, however, is sensitive to the type of ligand coordinated in the equatorial plane. When the equatorial ligands are capable of bidentate coordination, band II is approximately 445 nm, whereas with a ligand capable of only monodentate coordination, the value dropped to approximately 405nm.

The Rh_2^{4+} species prepared by Legzdins, et al.[3] is not an active hydrogenation catalyst in solution, though initial studies by Welty and Pinnavaia[9] have shown that Rh_2^{4+} is an active hydrogenation catalyst when exchanged onto the surfaces of H^+-hectorite.

The methanol solution of Rh_2^{4+} changes color from green to orange upon the addition of a saturated methanol solution of triphenylphophine. After some time, an orange solid precipitates from solution. This solid gives a chemical analysis which indicates that the complex has an empirical formula of $Rh(PPh_3)_3BF_4$. Conductivity measurements in nitromethane indicate that the complex is less than a 1:1 electolyte. This study indicates that the complex exists as an associated ion pair with a fluorine from the BF_4^- ion coordinated to the metal. When less concentrated solutions are prepared, $Rh(PPh_3)_3BF_4$ does not precipitate. Upon the addition of hydrogen, the phosphine complex solution changes color from orange to light yellow, which indicates that an oxidative addition of H_2 has occurred to form a hydride complex. No high field resonance for the metal hydride has been observed in the ^1H nmr spectrum. Treatment of the orange $Rh(PPh_3)_3BF_4$ solution with CO yields a complex, $Rh(CO)(PPh_3)_3^+BF_4^-$, which is a 1:1 electrolyte in nitromethane.

$Rh(PPh_3)_3BF_4$ is quantitatively converted to $RhCl(PPh_3)_3$ upon the addition of LiCl to the orange solution. The reaction of $Rh(PPh_3)_3BF_4$ with an excess of LiX is a general method of preparing $RhX(PPh_3)_3$. The complex obtained from the reaction of $Rh(PPh_3)BF_4$ and an excess of $Li(CH_3COO)$, $Rh(CH_3COO)(PPh_3)_3$, is a catalyst for the hydrogenation of alkenes and alkynes.[26]

The maximum rate of hydrogenation in the Rh_2^{4+}-PPh_3 system is obtained when the PPh_3:Rh ratio is equal to two. The catalyst is poisoned by O_2 and CO. Upon the addition of PPh_3 to Rh_2^{4+} exchanged onto a cation exchange resin, a heterogeneous hydrogenation catalyst is obtained.

The Rh_2^{4+}-PPh_3 system at a PPh:Rh ratio of 2 is also a catalyst for the hydroformylation of terminal olefins with a 1:1 mixture of H_2 and CO at 450 torr and 35°C. This same system is an effective catalyst for the carbonylation of methanol to acetic acid at 100°C and 25 atm of CO.[3]

Recently Wilson and Taube[21] have reported the synthesis of two Rh(II) dimers related to rhodium(II) acetate. These complexes, $Rh_2(CO_3)_4^{2-}$ and $Rh_2(SO_4)_4^{2-}$ were synthesized during attempts to prepare solutions of $Rh_2^{4+}{}_{(aq)}$ in high concentrations. The treatment of $Rh_2(CO_3)_4^{2-}$ with a strong non-complexing acid yielded a cationic species, $Rh_2(HCO_3)_2^{2+}$, but no Rh_2^{4+} was obtained. This species resembled the bis-μ-acetatodirhodium cation the authors found by protonating $Rh_2(CH_3COO)_4$ under the experimental conditions reported by Legzdins, et al.[3]

D. Previous Studies of Supported Homogeneous Catalysts

Most of the advantages of homogeneous and heterogeneous catalysis are combined by attaching homogeneous catalysts to inorganic (*ie*., silica gel, clay minerals) and organic (*ie*., polymers) matrices. Many research groups have become involved in the field of supported homogeneous catalysis in the hope of developing catalysts which might replace the traditional heterogeneous catalysts for industrial processes, and in the hope of gaining a better insight into the reaction mechanisms of catalysis.

The general means of preparing a supported homogeneous catalyst involves allowing the soluble catalyst to react with a functionalized support. The functional group is generally chemically similar to a ligand in the coordination sphere of the catalytically active metal atom. The reactions investigated to date involve a variety of hydrocarbon conversion reactions, which include hydrogenation, isomerization, hydroformylation, hydrosilation, acetoxylation, polymerization, and oligomerization.

The initial work in the field of supported homogeneous catalysis was reported in 1966, though there is some patent literature on the subject which dates back to 1940.[27,28] Acres, *et al*.[29] reported the impregnation of $RhCl_3$ in ethylene glycol into the pores of silica gel. This complex was active for the isomerization of 1-pentene. This procedure of preparing supported catalysts is the same as the one used to prepare liquid phase gas chromatography columns.

Rony[30] has reported the formation of a supported liquid phase catalyst (SLPC) for the hydroformylation of propylene on silica gel prepared with $RhCl(CO)(PPh_3)_2$ dissolved in butyl benzyl phthalate. The procedure for preparing the SLPC in both of these systems was to slurry the insoluble matrix in a volatile solvent and then add the homogeneous catalyst dissolved in sufficient nonvolatile solvent to just fill the pore volume of the solid support. Rony and Roth[31] recently have published a further investigation of SLPC systems in which they have expanded the types of catalysts supported by this method to include hydrogenation and isomerization catalysts. They also have reported that these catalysts may be impregnated into the support without the use of a nonvolatile solvent. This type of supported catalyst was refered to as a solid supported catalyst. For the hydroformylation of propylene and the isomerization of 1-butene, the SLPC was a more active catalyst when compared to the solid supported catalyst, but the opposite was true for the hydrogenation catalyst. No explanation was given for these results except that for some reactions a solvent must be present in order to obtain maximum activity.

Manassen[32] was one of the first to publish a report on binding transition metal catalysts to ion-exchange resins. By binding anionic and cationic metal salts or organometallic complexes of Group VIII metals to these resins, the author was able to examine catalytic carbonylation, hydroformylation, hydrogenation, isomerization, and transesterification.

The most studied form of heterogenizing a homogeneous catalyst has been to attach the soluble catalyst to an organic polymer, particularly polystyrene cross-linked with divinylbenzene.

Michalska and Webster,[33] and Pittman and Evans[34] have thoroughly reviewed the literature of polymer supported catalysts through 1973. These articles also include some studies in which silica was used as a support for homogeneous catalysts. In as much as this thesis deals with a rhodium hydrogenation catalyst, further discussion of other types of catalysts will not be included in this review unless information concerning these catalysts is pertient to this study or a novel approach to the problem of supported homogeneous catalysis is presented. Much of the work presented in the review articles is similar to the earliest work on this field except that a variety of catalysts and polymeric supports have been investigated.

Grubbs and Kroll[35] reported the attachment of a transition metal catalyst, $RhCl(PPh_3)_3$, to a 2% cross-linked polystyrene, which had been functionalized with a phosphine group.

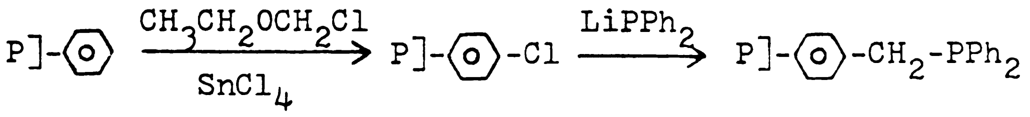

(5)

The soluble catalyst was allowed to equilibrate with the polymer for 2-4 weeks. This supported catalyst was active for the hydrogenation of olefins, and the rate of reduction depended on the molecular size of the olefin.

Grubbs, et al.[36] reported that as the polarity of the solvent increased, the catalyst became more selective for the reduction of polar substrates over nonpolar olefins. The absolute activity of this catalyst decreased by a factor of 0.06 when attached to the polymeric support as compared to the homogeneous analog.

Collman, et al.[37] have prepared a slightly different linkage for attaching the catalyst to the polymer.

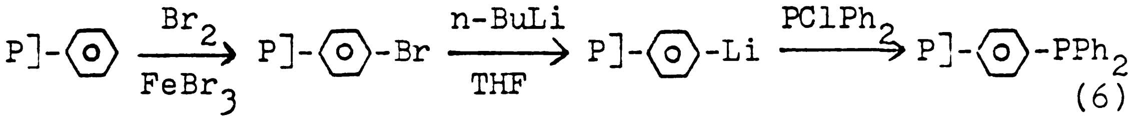

(6)

This likage is less basic that the one used by Grubbs and Kroll.[35] When $MCl(CO)(PPh_3)_2$ (M = Rh, Ir) was attached to the polymer, the authors showed that both phosphines in the complex were replaced by polymer attached phosphines. The polymer was mobile enough to bring two phosphines to close proximity of the metal for coordination.

For a catalytic reaction to occur, a vacant coordination site on the metal atom must be made available for the bonding of the substrate. There exist many monomeric complexes which could exhibit catalytic activity, but in solution the monomers dimerize. By attaching a monomeric complex to a rigid polymer, the combination of the monomers might be prevented. By employing this method, Grubbs, Brubaker and coworkers[38] were able to prepare a 20% cross-linked polystyrene supported monomeric titanocene dichloride. This species was reduced by n-butyl lithium to yield supported monomeric titanocene, which normally will dimerize in solution. This supported catalyst was six times more active for the hydrogenation of cyclohexene than the titanocene dimer in solution.

Dumont, et al.[39] reported the preparation of a supported chiral rhodium complex, similar to the soluble Rh(I)-diop complex[40] (diop = 2,3-O-isopropylidene-2,3-dihydroxy-1,4-bis(diphenylphosphino)butane) which is an asymmetric hydrogenation catalyst. The supported catalyst is much less active and gives lower optical yields than the homogeneous catalyst, but both the insoluble and soluble catlysts are equally efficient for the asymmetric hydrosilation of ketones.

Bruner and Bailar[41] have reported the synthesis of Pd(II) and Pt(II) dichloride complexes with polymeric diphenylbenzylphosphine as a ligand in the complex. These complexes are capable of reducing soybean methyl ester primarily to the monoene in nonpolar solvents. The initial composition of soybean methyl ester is 14.2% saturate, 22.3% monoene, 56.2% diene, and 7.0% triene. When methanol is used as the solvent, more reduction to the saturate occurs than when the reaction is carried out in nonpolar solvents.

A similar study, hydrogenation of polyenes to monoenes, has been published in which $RuCl_2(CO)_2(PPh_3)_2$ was used as the catalyst.[42] Pittman, et al.[43] have been able to attach this catalyst to a polymer. By using this supported catalyst, they obtained the same product yields and distributions that were obtained with the soluble catalyst.

In the same paper, Pittman, et al., reported that supported $Ni(CO)_2(PPh_3)_2$ was an effective cyclooligomerization catalyst, and that supported $RhH(CO)(PPh_3)_3$ was an effective hydrogenation catalyst. Also, the supported hydrogenation catalyst, the anchored analog of $RhCl(PPh_3)_3$, was examined in comparison to the soluble catalyst. When a finely divided (37-74µ) 1% cross-linked polystyrene was used as a support, the rate of hydrogenation was 0.8 times as fast as $RhCl(PPh_3)_3$ under 24 atm of H_2 and at 50°C. Grubbs, et al.[36] reported that the rate of hydrogenation with the insoluble catalyst was 0.06 times as fast as the homogeneous catalyst. An explanation for the difference between these two studies was that Grubbs used a less finely divided (74-149µ) 2% cross-linked polymer, and and the reaction was performed under less stringent conditions (1 atm and 25°C). When Pittman carried out the catalytic reaction with the 1% cross-linked polystyrene at 25°C, the rate was 0.5 times as fast as with the homogeneous catalyst.

Pittman and Smith[44] have reported the attachment of two catalytically active complexes to the same polymer, so that sequential multistep reactions can be catalyzed in the same system. They were able to anchor $Ni(CO)_2(PPh_3)_2$, a cyclooligomerization catalyst, and either $RhCl(PPh_3)_3$, a hydrogenation catalyst, $RhH(CO)(PPh_3)_3$, a hydroformylation catalyst, or $RuCl_2(CO)_2(PPh_3)_2$, a selective hydrogenation catalyst (vide supra), to the same polymer. With this system, the first step was to oligomerize butadiene to

4-vinylcyclohexene, 1,5-cyclooctadiene, and 1,5,9- cyclododecatriene, and then allow these products to interact with the second supported metal complex. It was impossible to compare the results of the supported catalysts to their homogeneous analogs because the reactions were carried out under different conditions.

Pittman and co-workers[45] have reported that at PPh_3:Ir ratios <5, the heterogeneous catalyst, derived from $IrCl(CO)(PPh_3)_2$, reduced 1,5-cyclooctadiene to cyclooctene at a rate faster than the corresponding homogeneous catalyst. At higher PPh_3:Ir ratios, the rates of hydrogenation for the homogeneous and heterogeneous catalysts were comparable. The supported catalyst also was capable of selectively hydrogenating 4-vinylcyclohexene to 4-ethylcyclohexene.[46]

Much of the earliest work in supported catalysis was done by researchers in the labs of British Petroleum, and published only in the patent literature.[33] Recently this work has been published in the open literature.[47-49] It was found that a supported catalyst, prepared from a reaction between phosphinated polystyrene and $Rh(acac)(CO)_2$, was active for the hydroformylation of 1-hexene, and $[RhCl(C_8H_{12})]_2$ anchored on an identically prepared polymer was a catalyst for the hydrogenation of 1-hexene and cyclohexene. For the hydrogenation reaction, more forcing conditions (50°C and 15atm of H_2) were required than those reported by Grubbs and Kroll.[35] The authors were also able to anchor $Ni(C_8H_{12})_2$ to a phosphinated polystyrene which was an oligomerization catalyst for butadiene. Diethyl aluminum ethoxide was required as a cocatalyst for this last reaction. All of these reactions were performed in a fixed bed reaction vessel with liquid feedstocks.[47]

Silica gel may also be functionalized with a variety of reagents, by using the available surface Si-OH groups. Two general procedures have been reported for anchoring of the catalyst to silica.[48,49] In the first method silica was treated with (2-diphenylphosphinoethyl)triethoxysilane, which yielded a functionalized silica:

$$Ph_2PCH_2CH_2Si - (O)_3 - \text{ silica}$$

The functionalized silica was then allowed to react with the catalyst precursor. The second method involved the synthesis of the catalyst with (2-diphenylphosphinoethyl)triethoxysilane used in place of triphenylphosphine. The product was then allowed to react with the silica. The advantage the second method has over the first was that the phosphine:metal ratio could be controlled to a greater extent. By these methods, phosphine complexes of rhodium, iridium, ruthenium, and platinum have been chemically bonded to silica. Complexes of the first three metals were prepared by the second method, and a platinum complex was prepared by the first. All of these complexes were active for the hydrogenation of olefins and dienes.[48,49] No rate data were presented, so a comparison between the supported catalyst and the analogous homogeneous catalyst was not possible.

Boucher and co-workers[50] have anchored Rh(I) and Co(II) phosphine complexes through silane linkages to silica. The silane linkages were formed by allowing trichlorosilylalkylphosphines, acyloxysilylphosphines, or alkyloxysilylphosphines to react with the surface Si-OH groups of silica. A variety of Rh(I) chloro complexes or $Co(acac)_2$ were then allowed to react with the functionalized silica. These heterogeneous complexes were catalysts for the hydroformylation of propylene. The cobalt complex was less active than the rhodium species. In comparison to $RhCl(PPh_3)_3$, the analogous heterogeneous species was 1.4 times more active than the soluble catalyst.

Recently, Bayer and Schurig[51] have reported the formation of a soluble supported catalyst prepared with a non-cross-linked polystyrene in a manner similar to the one used by Collman, et al.[37] The catalyst and products were separated easily by molecular weight differences. By this method the authors were able to prepare catalysts analogous to $RhCl(PPh_3)_3$ and $RhH(CO)(PPh_3)_3$ with polymeric phosphine ligands. The advantage this system has over the insoluble polymer catalysts is that as in solution all the active sites are equally accessible to the reactants.

Parshall[52] has reported a novel method of preparing a catalyst which is easily separated from the reaction products. By dissolving $PtCl_2$ in low-melting tetraalkylammonium salts of $SnCl_3^-$ and $GeCl_3^-$, a catalytic system was obtained that was active for the hydrogenation , isomerization, hydroformylation, and carbonylation of olefins. For the hydrogenation of 1,5,9-cyclododecatriene, considerable selectivity to the monoene was obtained with this catalyst. The products were separated from the catalyst by distillation or decantation. The salts were found to act as stabilizing ligands, thus preventing the formation of platinum metal.

II. EXPERIMENTAL

A. Reagents and Solvents

Hectorite and Wyoming montmorillonite were obtained from the Baroid Division of NL Industries as the spray-dried sodium form. The hectorite contained a $CaCO_3$ impurity which was removed by reaction with HSO_4^-(see section on Infrared Spectra) before use in the spectroscopic studies. The $CaCO_3$ was not removed from the mineral prior to use in the hydrogenation studies. $RhCl_3 \cdot 3H_2O$, with a reported Rh assay of 42.82%, was purchased from Engelhard Industries. Triphenylphosphine, 3-butyn-1-ol, 3,3-dimethyl-1-butene, 1-heptene, 1,5-hexadiene, 2-hexene (cis and trans mixture), phenyl acetylene, and propargyl chloride were purchased from Aldrich. Allyl phenyl ether, 1-hexene, 1-hexyne, 2-hexyne, and 1-octyne were purchased from Pfatz and Bauer. Cyclohexene, 2-methyl-3-butyn-2-ol, propargyl alcohol, and 48% fluoroboric acid were purchased from J. T. Baker; and allyl alcohol was purchased from Fisher Scientific. Dimethylphenylphosphine was purchased from Research Organic/Inorganic Chemical Corporation. All unsaturated substrates were distilled under argon prior to use, into a graduated reservoir before being added to the reaction flask. Triphenylphosphine was used without further purification. A 0.05M triphenylphosphine solution in methanol was prepared for use in the catalytic studies.

Methanol, used in determining the activity of the mineral-bound catalyst, was purchased from Matheson, Coleman and Bell. The water content in the methanol was reported as 0.2%. If methanol is obtained with less than 0.1% water, no catalytic reaction is observed. Also, when methanol is stored over CaH_2 and distilled before use in the catalytic reaction, no activity is observed. All methanol is deaereated under a stream of dry nitrogen for 30 minutes before being stored in the dry box. All exchange reactions were carried out under oxygen-free conditions in a dry box with a dry nitrogen atmosphere.

In all hydrogenation reactions, oxygen was rigorously excluded. Bottled hydrogen (Airco) was passed through a BTS catalyst at 120-130°C, and then through a bed of Aquasorg (Mallinkrodt Chemical Works) before being passed through the hydrogenation apparatus. Bottled argon (Airco) and nitrogen (Airco) were used without treatment.

Microanalyses were performed by Galbraith Laboratories, Inc., Knoxville, Tennessee.

B. Syntheses

1. Methanol Adduct of Tetrakis-μ-acetatodirhodium(II)

The procedure for the preparation of rhodium(II) acetate was modified from literature methods.[52] Rhodium trichloride trihydrate (5.0g) and sodium acetate trihydrate (10.0g) in glacial acetic acid (100ml) and absolute ethanol

(100 ml) were allowed to reflux for two hours. The initially red solution became green, and a green solid precipitated. After the solution was cooled to room temperature, the solid was collected by filtration on a glass frit. The crude product was dissolved in 600 ml of boiling methanol, and filtered. The solution was concentrated to 400 ml and refrigerated at 0°C overnight. The methanol adduct was collected by filtration. The overall yield was 3.62g (75% based on $RhCl_3 \cdot 3H_2O$). The infrared spectrum of the complex was identical to the spectrum of anhydrous $Rh_2(CH_3COO)_4$ reported in the literature[54] with the exception of the bands which are due to coordinated methanol (ν = 2980 and 2935 cm^{-1}). The electronic spectrum of the complex in methanol (λ_{max} = 586 and 445 nm) was also similar to the spectrum of the reported complex in ethanol (λ = 590 and 446 nm).[3]

2. Protonation of $Rh_2(CH_3COO)_4 \cdot 2CH_3OH$

Protonation of rhodium(II) acetate by tetrafluoroboric acid was carried out in a water-methanol solution. The product, $Rh_2(CH_3COO)_{4-x}{}^{x+}$ (x = 1 or 2), could not be precipitated by any known anion. The stock solution, which was used in preparing the rhodium exchanged minerals, was prepared by placing 1.2g of $Rh_2(CH_3COO)_4 \cdot 2CH_3OH$ (2.4 mmoles) in 300 ml of methanol and adding 1.32 ml of aqueous 48% tetrafluoroboric acid (9.7 mmoles). The mixture was heated and stirred in an oil bath at 60°C, until the green solid dissolved (approximately 2 days). The concentration of this green solution was 0.008M. The uv-visible spectrum of the protonated product, $Rh_2(CH_3COO)_{4-x}^{x+}$ (λ_{max} = 615 and 427 nm), was similar to the spectrum for Rh_2^{4+} reported by Legzdins, *et al.*[3] (λ_{max} = 612 and 423 nm).

3. Exchanged Hectorites

Hectorite was chosen as the primary mineral to be used as a support for the catalysts investigated in this work. This mineral has a reported cation exchange capacity (CEC) of 95.5 meq/100g,[55] however an independant determination of the CEC by a conductometric titration of a Cu^{2+}-saturated hectorite with NaOH in a ethanol-water solution gave a value of 70 meq/100g.[56] This value is in agreement with the one obtained by chemical analysis (2.05% Cu) of a Cu^{2+}-saturated hectorite. Therefore, the CEC of the mineral was taken to be 70 meq/100g.

a. $Rh_2(CH_3COO)_{4-x}^{x+}$-Hectorite

Ten milliliters of the stock 0.002*M* solution of $Rh_2(CH_3COO)_{4-x}^{x+}$ was allowed to react with 0.5g of hectorite. The slurry was stirred on a medium glass frit for 1-2 minutes, then the solution was filtered off. Upon treatment with the rhodium complex, the white mineral became emerald green in color, while the color of the solution became less intense. The clay was then washed six times with methanol to remove excess $Rh_2(CH_3COO)_{4-x}^{x+}$, and the mineral was dried under N_2. Chemical analysis (0.76% Rh, 7.4 mmoles/100g) indicated that $Rh_2(CH_3COO)_{4-x}^{x+}$ occupied approximately 12% of the exhange sites in the mineral. This was the general procedure used for the catalytic studies, but the amount of rhodium complex exchanged onto the mineral could be increased by prolonged contact between the solution and the mineral and by using a higher concentration of the rhodium solution. For all the catalytic studies, the $Rh_2(CH_3COO)_{4-x}{}^{x+}$-hectorite was prepared within a week of use because a reduced activity was observed after the mineral had aged longer than this period. (approximately 25% of the activity was lost)

An analogously exchanged mineral, $Rh_2(C_6H_5COO)_{4-x}{}^{x+}$-hectorite was prepared with the product of the protonation of $Rh_2(C_6H_5COO)_4$. Rhodium(II) benzoate was prepared according to literature methods.[13]

b. $Rh(PPh_3)_x{}^+$-Hectorite

A 0.2g sample of $Rh_2(CH_3COO)_{4-x}{}^{x+}$-hectorite was allowed to react with varying amounts of a 0.05M PPh_3 solution so that the PPh_3:Rh ratio was in the range of two to fourteen. The color of the mineral immediately changed color from green to dark orange upon the addition of PPh_3. Similar reactions were obtained when diphenylmethylphosphine[57] and dimethylphenylphosphine were used in place of PPh_3. This type of reaction is indicative of the formation of a Rh(I) species. The maximum rate of hydrogenation was found to occur with a PPh_3:Rh ratio of nine. The concentration of the phosphine in the reaction mixture was 4.6mM.

When PPh_3 was allowed to react with $Rh_2(C_6H_5COO)_{4-x}{}^{x+}$-hectorite, a reaction similar to the one with the acetate complex was observed.

C. Physical Methods

1. Gas Chromatography

Gas phase chromatography of liquid and vapor samples was performed with a Varian Associates Model 90-P single column chromatograph with a thermal conductivity detector. The output of the detector was recorded with a Sargent Model SR recorder.

Olefin-alkane and alkyne-alkene-alkane separations were achieved by use of a 5' x ¼" stainless steel column packed with 3% SE-30 on diatomite CLQ 100/120. The column was operated at 30°C and at a flow rate of 30 ml/min. Helium was used as the carrier gas.

A 0.6 ml vapor sample or a 1.6 μl liquid sample was injected into the chromatograph to obtain optimum identification of the components in the sample.

2. X-Ray Diffraction Studies

Basal spacings (001) for the rhodium exchanged mineral samples were determined by x-ray diffraction with a Phillips x-ray diffractometer with Ni-filtered Cu K(α) radiation. The minerals were deposited on microscope slides from a methanol slurry and the solvent was allowed to evaporate. Self-supporting film samples were also useful for determining 001 spacings. The films were placed on microscope slides in a small plastic bag with methanol added. The bag was then heat sealed before the basal spacings were measured. This procedure allowed the 001 spacings to be measured on a fully solvated and swelled minerals, and it prevented the sample from coming in contact with air. The diffractions were monitored through 14° of 2θ. The peak positions in degrees of 2θ were converted to d-spacings with a standard chart.

3. UV-Visible Spectra

UV-Visible spectra of solutions were obtained in 1 cm path length matching quartz cells with either an Unicam Model SP 800B spectrophotometer or a Cary 17 spectrophotometer. Electronic spectra of clay samples were recorded by use of a Cary 17 spectrophotometer. The solid samples were prepared by mulling the clay samples in mineral oil and by placing the mull between two Infrasil 2 quartz disks. In the reference beam was placed a mull sample of native hectorite in order to reduce the effects of scattering.

4. Infrared Spectra

Infrared spectra were recorded by use of a Perkin-Elmer Model 457 grating spectrophotometer. The samples were prepared by mulling in Fluorolube (Hooker Chemical Co.) then placing the mulls between CsI plates. Some clay samples were examined as self-supporting films. The ir spectrum of native hectorite (*cf*. Figure 3b) exhibited a broad peak centered at 1440 cm^{-1} which was assigned to a $CaCO_3$ impurity. This impurity was removed by treating hectorite with $NaHSO_4 \cdot H_2O$.

The mineral (4.0g) was washed twice with 0.1*M* sodium bisulphate solutions (100 ml each). The clay was rinsed with water and the wash solution was tested with a $BaCl_2$ solution to insure the complete removal of SO_4^{2-}. The mineral was then washed with a 1.0*M* NaCl solution, rinsed, and

Figure 3. Infrared Spectra of Na^+-Hectorite; (a) After Treatment with Sodium Bisulfate to Remove Calcium Carbonate Impurity, (b) Before Treatment with Sodium Bisulfate.

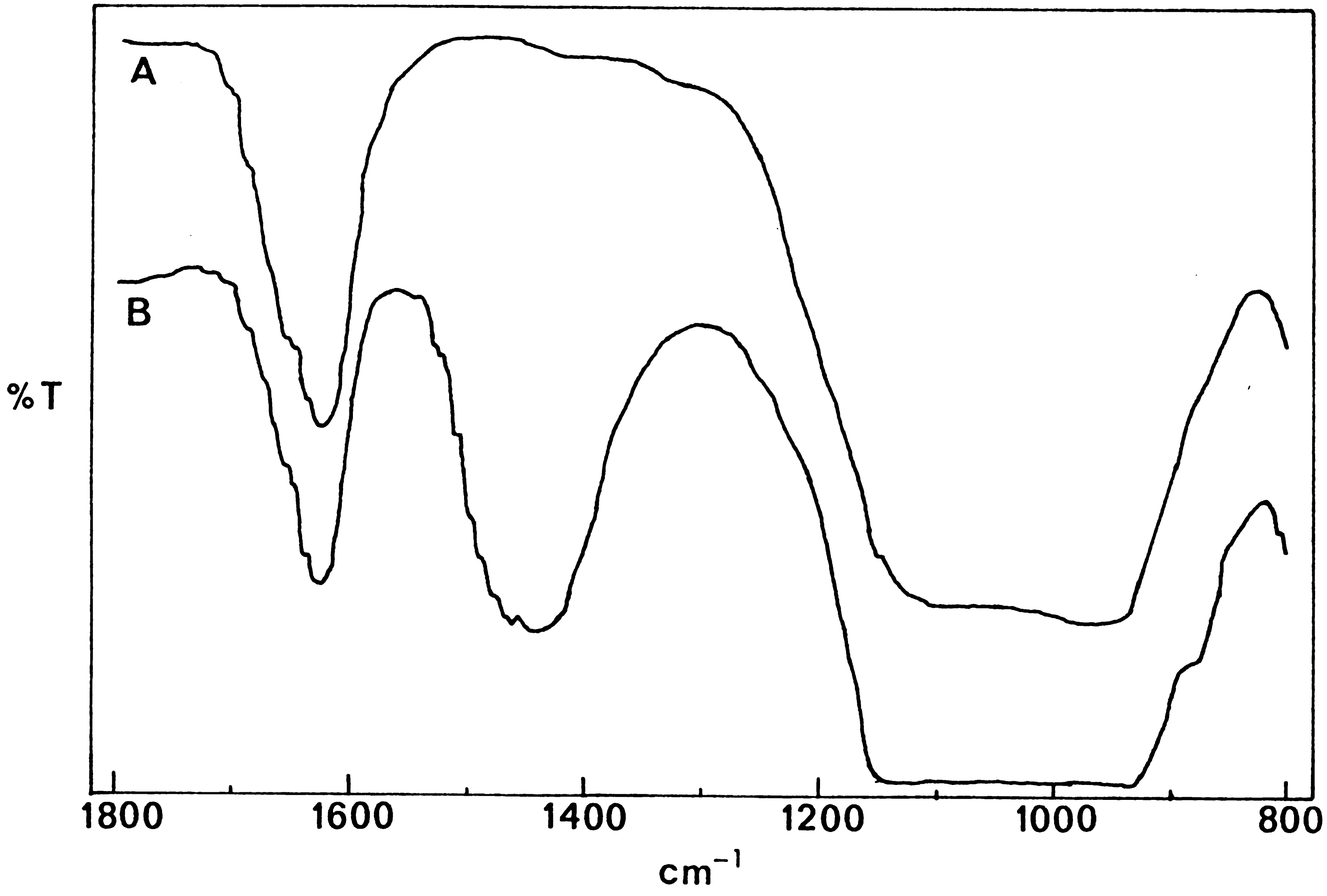
A
B
%T
1800
1600
1400
1200
1000
800
cm^{-1}

freeze-dried. This treatment completely removed the impurity band (*cf*. Figure 3a).

5. Proton NMR Studies

Proton magnetic resonance spectra were obtained by use of a Varian Associates A56/60D analytical spectrometer which operates at a frequency of 60.000 MHz. The spectra were recorded either in the normal mode, or in the case of very dilute samples, with the aid of a Varian Associates C-1024 time averaging computer. All spectra were recorded at field strengths well below the level required to produce saturation. Chemical shifts were measured by using tetramethylsilane as an internal standard, or by using sodium 3-trimethyl silyl-2,2,3,3-d_4-propionate in D_2O (5% w/v) as an external standard.

6. Phosphorus-31 NMR Studies

Phosphorus-31 nmr spectra were recorded on a Brüker HFX-10 spectrometer modified for multinuclear measurements as descibed by Traficante, *et al*.[58] and equiped with a Nicolet 1083 computer with 12K of memory, a Diablo disc memory unit, and a Nicolet 293 I/O controller. The spectra were obtained at a frequency of 36.442 MHz.

All samples were dissolved in methanol with 30% hexafluorobenzene added to serve as an internal fluorine-19 lock. The spectra were measured over 5000 Hz (137 ppm) spectral width. Optimum signal-to-noise was obtained by using between 512 and 1024 scans per spectrum. Chemical shifts were measured by using a 85% H_3PO_4 solution as an external standard.

D. Hydrogenation Studies

Hydrogenation rates were measured as the rate of hydrogen consumption at constant pressure and under ambient conditions. A schematic of the hydrogenation apparatus is shown in Figure 4. The reaction flask was specially designed with the help of Mr. Andrew Seer, a master-glassblower in this department, to prevent the splashing of the catalyst onto the walls of the flask (cf. Figure 5).

The general procedure for obtaining hydrogenation rates at 25°C was to place 0.2g of $Rh_2(CH_3COO)_{4-x}^{x+}$-hectorite into the reaction flask, and then to add sufficient deareated methanol so that after the addition of the required amount of 0.05M triphenylphosphine solution, and substrate, the total volume of the reaction mixture was 30 ml. After the addition of triphenylphosphine, the flask was removed from the dry box and connected to the hydrogenation apparatus. The system, with the exception of the reaction flask, was purged with hydrogen for a minimum of 10 minutes. The mercury levels in both the manometer and gas measuring tube were then manipulated to insure complete purge with H_2. The manometer and gas measuring tube were isolated from the rest of the system. The manifold was then evacuated and filled with H_2. This cyclic process was repeated three times, and then a similar procedure was applied to the reaction flask. The flask was opened to the rest of the system along with the manometer and gas measuring tube, and H_2 was bubbled through the stirred methanol slurry for two hours to

Figure 4. Schematic of Hydrogenation Apparatus

a) Reaction Flask
b) Condensor
c) Apparatus for the Distillation of the Substrates
d) Manometer
e) Gas Measuring Tube and Leveling Bulb

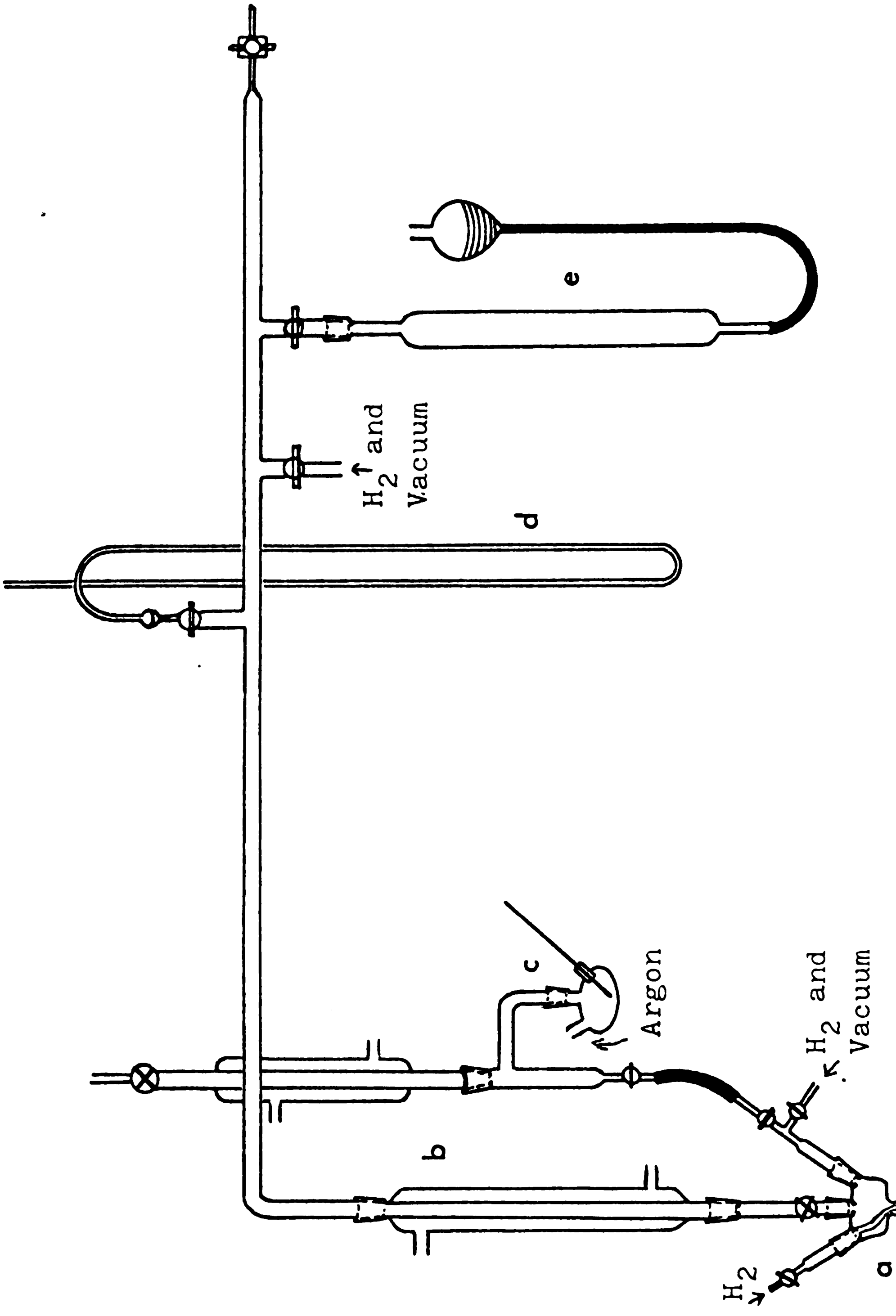
H_2 and Vacuum
e
d
c
Argon
b
H_2 and Vacuum
a
H_2

Figure 5. Reaction Flask with Adaptors for Connecting to the Hydrogenation Apparatus

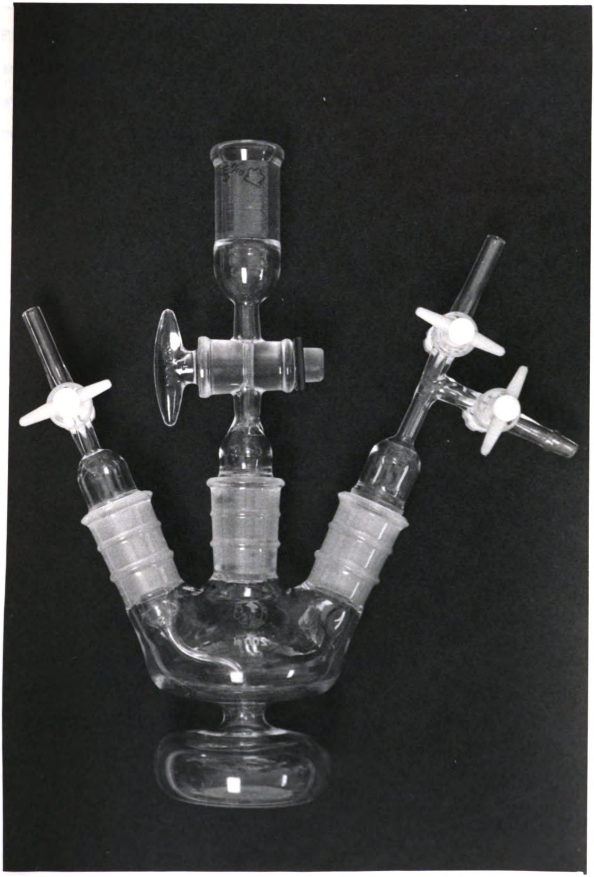

allow time for the formation of the active hydride species. Finally, the substrate was distilled and added to the reaction mixture. The rate of H_2 consumption was monitored over 15-20% of the reaction for alkenes, and 40-50% of the reaction for alkynes.

III. RESULTS AND DISCUSSION

A. Characterization of the Homogeneous Catalyst

1. Solution Chemistry of $Rh_2(CH_3COO)_{4-x}{}^{x+}$ (x = 1,2)

When Legzdins, *et al.*[3,22] reported the protonation of $Rh_2(CH_3COO)_4$ with a strong non-complexing acid, HBF_4, the authors believed that they had obtained a totally protonated species, $Rh_2{}^{4+}$, with all four of the acetate ligands removed from the coordination sphere. Analysis of free acetate, as acetic acid and methyl acetate, by glc methods indicated that all acetate ligands were lost upon protonation. They also reported that the ion prepared was not air sensitive. $Rh_2(CH_3COO)_4$ is similar to $Mo_2(CH_3COO)_4$ and $Re_2(CH_3COO)_4Cl_2$, which are complexes with strong metal-metal bonds. These latter two complexes are protonated by hydrochloric acid to give $Mo_2Cl_8{}^{3-}$ and $Re_2Cl_8{}^{2-}$. Bridged acetate complexes of Cu(II) and Cr(II), when protonated with strong acid, give monomeric species. This behavior is indicitive of a weak metal-metal bond in the complex. The stability of copper(II) acetate and chromium(II) acetate is due solely to the four bridging acetate ligands.

Maspero and Taube[17] also reported the formation of $Rh_2{}^{4+}$, prepared from the reduction of Rh(III) by Cr^{2+}. The electronic spectrum of this ion differed from the one reported by Legzdins, *et al*.[3] This ion was very air-sensitive. With both preparations, no counterions could be found to precipitate a simple salt.

Wilson and Taube[23] repeated the experiment of Legzdins, *et al*.[3] and found that only one or two acetate ligands was removed from the coordination sphere by protonation. Their conclusions are based on ion-exchange chromatography. They were able to separate a species with a +1 charge, and another with a +2 charge. Figure 6 shows the probable products which were isolated by this experiment.

In order to obtain more information on the products of the protonation of rhodium(II) acetate, the ^1H nmr spectrum of the reaction products was recorded. A 0.01*M* solution of $Rh_2(CH_3COO)_{4-x}^{x+}$ was prepared in a manner identical to the procedure used in the catalytic studies. The pmr spectrum (*cf*. Figure 7) of this dilute solution was recorded with the aid of a time averaging computer. The peak at 1.99 ppm has been assigned to the methyl protons of the acetate moiety in methyl acetate. Methyl acetate is the only form of uncoordinated acetate found in the product mixture. The equilibrium between acetic acid and methyl acetate in the acid catalyzed esterification of acetic acid is shifted completely to the ester since there is a large excess of methanol present in the reaction mixture.

$$CH_3COOH + CH_3OH \xrightleftharpoons{H^+} CH_3COOCH_3 + H_2O \qquad (7)$$

The methyl resonance for the ester group was observed at 3.61 ppm. The pmr spectrum of acetic acid (15 μl) in

Figure 6. Possible Products of the Protonation of Rhodium(II) Acetate; (a) Rhodium(II) Acetate, (b) *Tris*(acetato)dirhodium(II), (c) *Trans*-*bis*-(acetato)dirhodium(II), (d) *Cis*-*bis*(acetato)-dirhodium(II)

Figure 7. ^{1}H NMR Spectrum of the Products of the Protonation of Rhodium(II) Acetate Performed in a Sealed NMR Tube

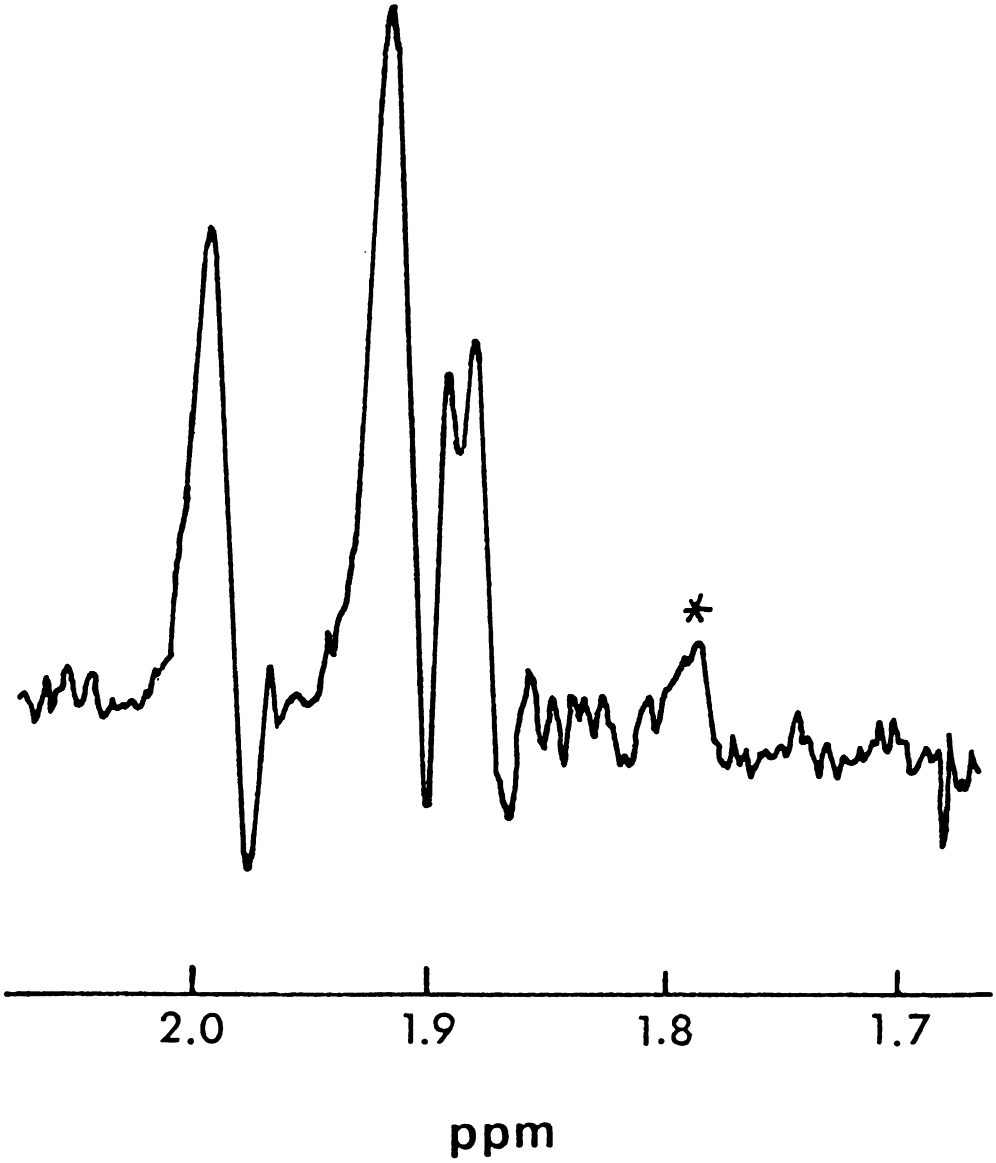
*
2.0
1.9
1.8
1.7
ppm

methanol (1 ml), with 5 µl of 48% aqueous HBF_4, exhibits two peaks of equal intensity, at 1.99 ppm and 3.61 ppm. These values agree with the reported values of 2.00 and 3.65 ppm for methyl acetate.[59] When the protonation reaction is performed in 48% aqueous HBF_4, with no methanol present, acetic acid is the only uncoordinated acetate product observed by pmr. In Figure 7, the other three resonances in the acetate region, with approximate relative intesities of 2:1:1, are assigned to the remaining coordinated acetate ligands. Planimetric integration of the peaks observed from the protonation reaction showed that the ratio of coordinated to uncoordinated acetate is 2.2:1. This value indicates that a mixture of tris- and bis-(acetato)dirhodium(II) exists in solution with the tris-complex being the predominant species in the product mixture (3 tris-:1 bis-). If only the tris-complex were present the ratio of the coordinated to uncoordinated acetate would be 3:1, whereas if the only the bis-complex were formed, the ratio would be 2:2.

The uv-visible spectrum for the protonated product mixture, along with the previously reported spectra for related Rh(II) species are presented in Table 1. In the visible region of the spectrum, all the species exhibit two absorptions; band I at approximately 600 nm, and band II in the region of 400 to 450 nm. Band I is particularly sensitive to changes in the axial ligands, while band II is insensitive to changes in these ligands.[24] Band II, however, seems to be sensitive to the presence of bridging ligands in the coordination sphere of the complex. Band I also is sensitive to the number of bridging acetate ligands. The values for the rhodium(II) acetate complexes range from 586 nm for the complex with four coordinated acetate ligands, to 648 nm for a complex without bridging acetate ligands. A bathochromic shift in band I was observed as the protonation reaction proceeded. At the end of the reaction the value for this band was intermediate to that reported for $Rh_2(CH_3COO)_3^+$ and $Rh_2(CH_3COO)_2^{2+}$ (*cf*. Figure 8 and Table 1). Again it is resonable to postulate that both $Rh_2(CH_3COO)_3^+$ and $Rh_2(CH_3COO)_2^{2+}$ exist in the product mixture.

The nmr and electronic spectra show indeed that acetate ligands remain in the coordination sphere of the dirhodium(II) moiety after protonation of $Rh_2(CH_3COO)_4$, as has been reported by Wilson and Taube.[23]

2. Solution Chemistry of $Rh(PPh_3)_3BF_4$

The interaction of the green-colored $Rh_2(CH_3COO)_{4-x}^{x+}$ solution at a concentration of $8x10^{-3}$M with triphenylphosphine yielded an orange solution which in the presence of hydrogen was an active catalyst for the hydrogenation of alkenes and alkynes, hydroformylation of alkenes, and carbonylation of methanol to acetic acid and methyl acetate. The proton nmr spectra of the reactant solution and the product solution are shown in Figure 9. Spectrum A is similar to the spectrum presented in Figure 7, and B is the spectrum of the solution after the addition of PPh_3. Triphenylphosphine was added so that the PPh_3:Rh ratio was equal to 3.5:1.

Figure 8. Visible Spectra Which Show the Progress of the Protonation of Rhodium(II) Acetate; (1) After 14 Hours, (2) After 23 Hours, (3) After 41 Hours, (4) After 112 Hours

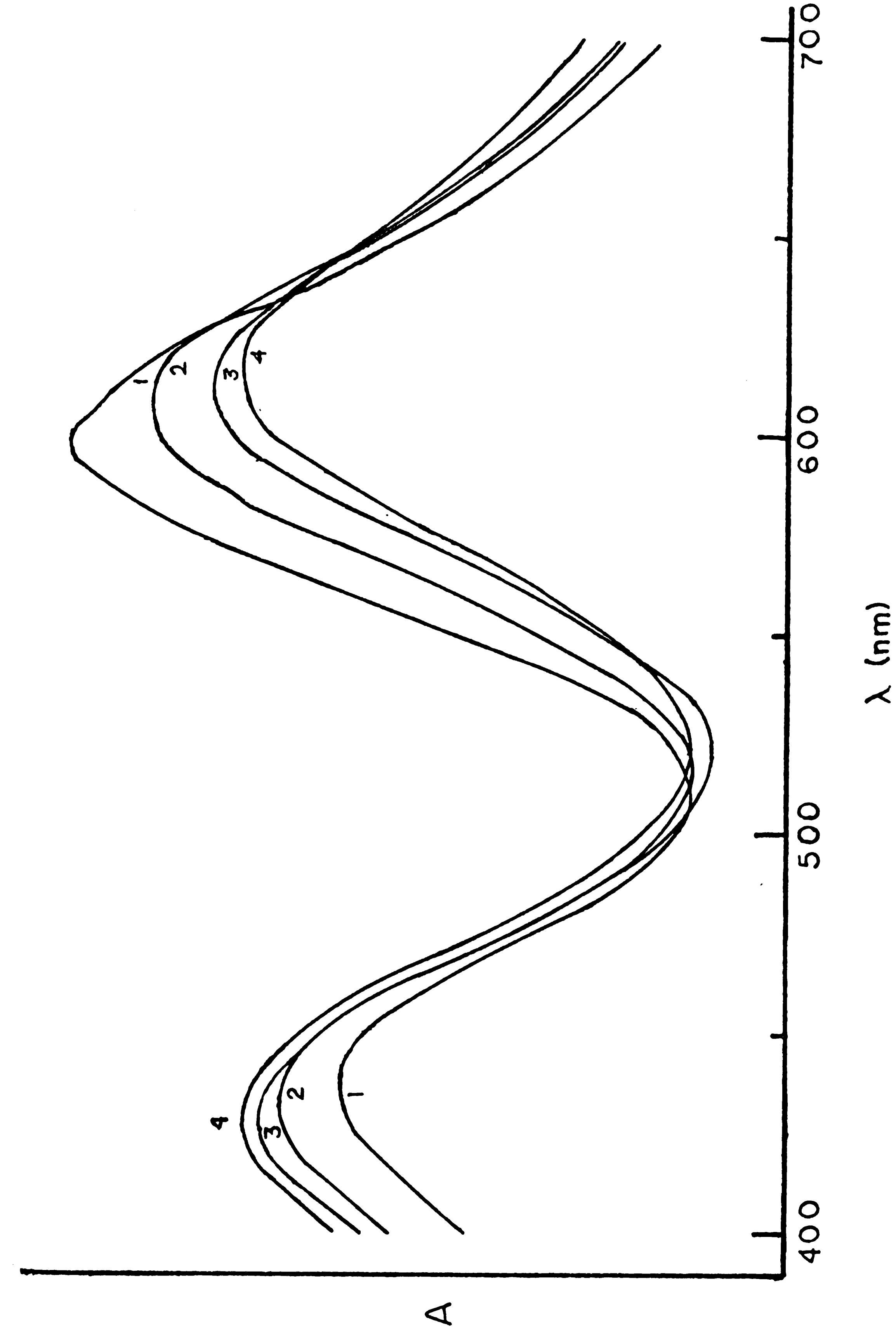
A
λ (nm)
400
500
600
700
1
2
3
4
1
2
3
4

Table 1. UV-Visible Spectrometric Data

Species	Band I[a]	Band II[a]	Other Bands	Conditions
$Rh_2(CH_3COO)_{4-x}{}^{x+}$ [b]	615 (131)	429 (131)	350sh, 258	HBF_4 in methanol-H_2O
$Rh_2(CH_3COO)_4$	585 (241)[c] 587[c] 586[b]	440 (106) 443 445	250, 218	in H_2O in ethanol in methanol
$Rh_2(CH_3COO)_3{}^{+}$ [d]	610	425	350sh, 250, 218	in HTFMS[e] and $HClO_4$
$Rh_2(CH_3COO)_2{}^{2+}$ [d]	638 (71)	423 (99)	368, 258, 220	1M $HClO_4$
Legzdins' species[c]	612 (55)	423 (62)	256	HBF_4 in methanol-H_2O
$Rh_2{}^{4+}$	648 (93)[d] 630 (80)[f]	402 (126) 412 (118)	250 250	1M $HClO_4$ 3M $HClO_4$
$Rh_2(C_6H_5COO)_{4-x}{}^{x+}$ [b]	603	437		HBF_4 in methanol-H_2O

a) Values in parentheses are molar absorptivities

b) Work performed in this study

c) Reference 3

d) Reference 22

e) Reference 16

f) HTFMS = trifluoromethylsulfonic acid

Figure 9. ^{1}H NMR Spectra of (a) Products of the Protonation of Rhodium(II) Acetate, (b) The Same Solution After the Addition of Triphenylphosphine

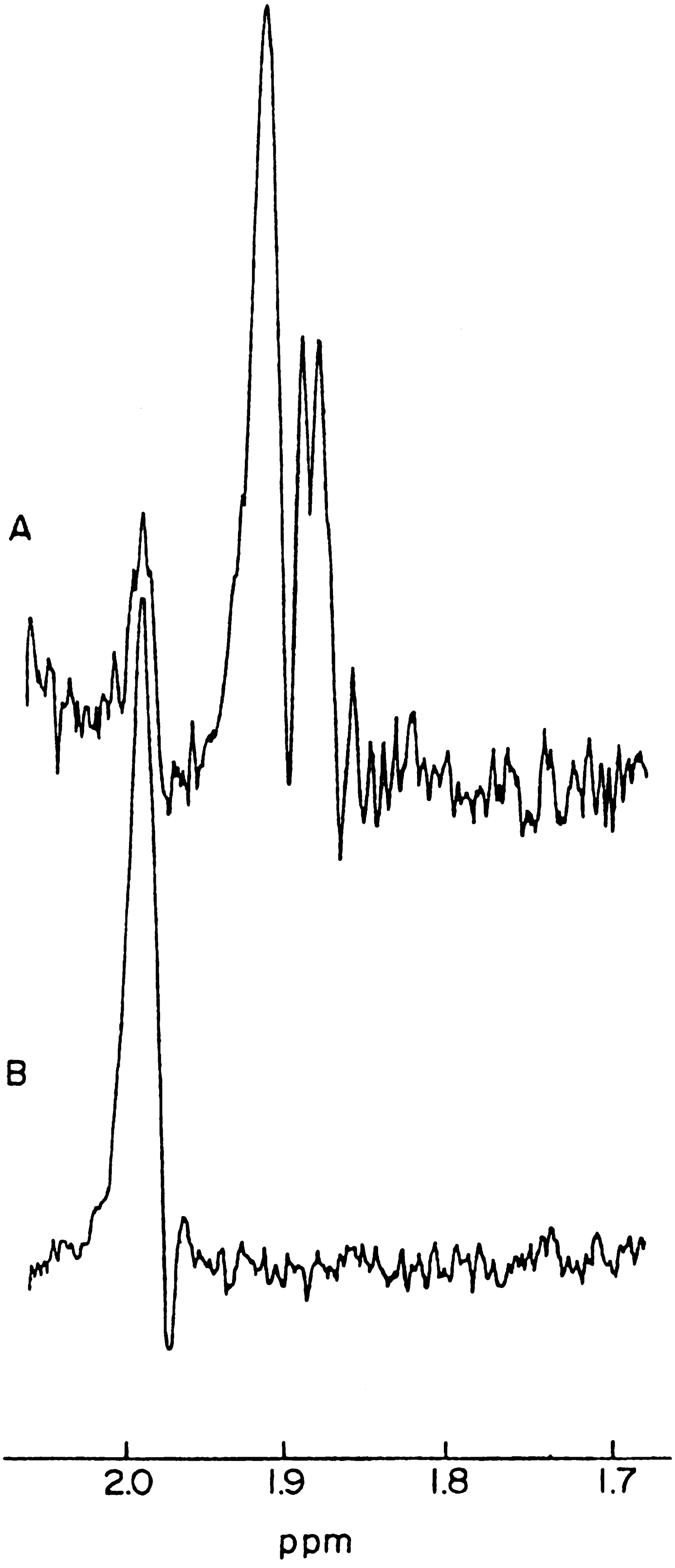
A
B
2.0
1.9
1.8
1.7
ppm

Spectrum B shows that upon the addition of the phosphine, all the resonances which are assigned to coordinated acetate disappear while the resonance which is assigned to methyl acetate increases.

In order to obtain a better understanding of the rhodium-phosphine interaction, a ^{31}P nmr investigation was undertaken. The standard $Rh_2(CH_3COO)_{4-x}{}^{x+}$ solution ($8x10^{-3}$M) was concentrated by rotoevaporation to $8x10^{-2}$M so that the phosphorus signal would be observable with a resonable number of transients.

When triphenylphosphine, tri-(p-tolyl)phosphine, or diphenylmethylphosphine was added to the concentrated rhodium(II) solution so that the P:Rh ratio was equal to 3.5:1, an immediate precipitation of orange crystals occurred. A P:Rh ratio of 3.5 instead of 3 was used because it was likely that the phosphine was acting as the reducing agent for the reaction. Triphenylphosphine is known to be the reducing agent in the reduction of $Rh_2(CH_3COO)_{4-x}{}^{x+}$ to $Rh(CH_3COO)(PPh_3)_3$ in the presence of excess lithium acetate and triphenylphosphine.[26] The phosphine is oxidized to the corresponding phosphine oxide. The precipitate from the reaction of $Rh_2(CH_3COO)_{4-x}{}^{x+}$ and dimethylphosphine was analyzed and it was found to have the empirical formula, $Rh(PPh_2CH_3)_3BF_4$, which is similar to the related triphenylphosphine complex.[3] When dimethylphenylphosphine was the phosphine used in the reaction, no precipitate was observed at a P:Rh ratio of 3.5. It was assumed that the species formed was similar to the related PPh_3 and PPh_2CH_3 complexes.

The proton decoupled ^{31}P nmr spectrum obtained from the product of the reaction between $PPh(CH_3)_2$ and $Rh_2(CH_3COO)_{4-x}{}^{x+}$ is shown in Figure 10. It consists of a doublet at +5.9 ppm and a doublet of doublets centered at -5.2 ppm, and a singlet at -39.2 ppm. The latter line is assigned to the phosphine oxide. The splitting of coordinated ligand resonances due to P-P coupling was not observed because the solution could not be cooled without precipitation of the complex. The larger splitting is due to ^{103}Rh-^{31}P coupling, and the smaller splitting (26 Hz) arises from an unknown source. One possibility for the smaller splitting is coupling of the phosphorus in the trans position (cf. Figure 11) to fluorine in the tetrafluoroborate ion. Previouly, an ion pair has been suggested to exist between the anion and the metal complex.[3] However, the ^{19}F nmr spectrum exhibits only a singlet for the BF_4^- ion. A doublet with a splitting of 26 Hz would be expected if the fluorine were coupled to a phosphorus. The resonance in the ^{19}F nmr spectrum of the BF_4^- is shifted downfield by 2 ppm as compared to the signal due to $NaBF_4$ in methanol (Hexafluorobenzene was used as an internal standard.). A downfield shift would be expected if the tetrafluoroborate ion were associated with the rhodium complex. The absence of ^{103}Rh-^{19}F coupling and ^{31}P-^{19}F coupling for BF_4^- suggest that the lifetime of the ion in the coordination shere of the metal must be short. The nmr data are compiled in Table 2.

Figure 10. ^{31}P NMR Spectrum of $Rh(PPh(CH_3)_2)_3BF_4$ in Methanol

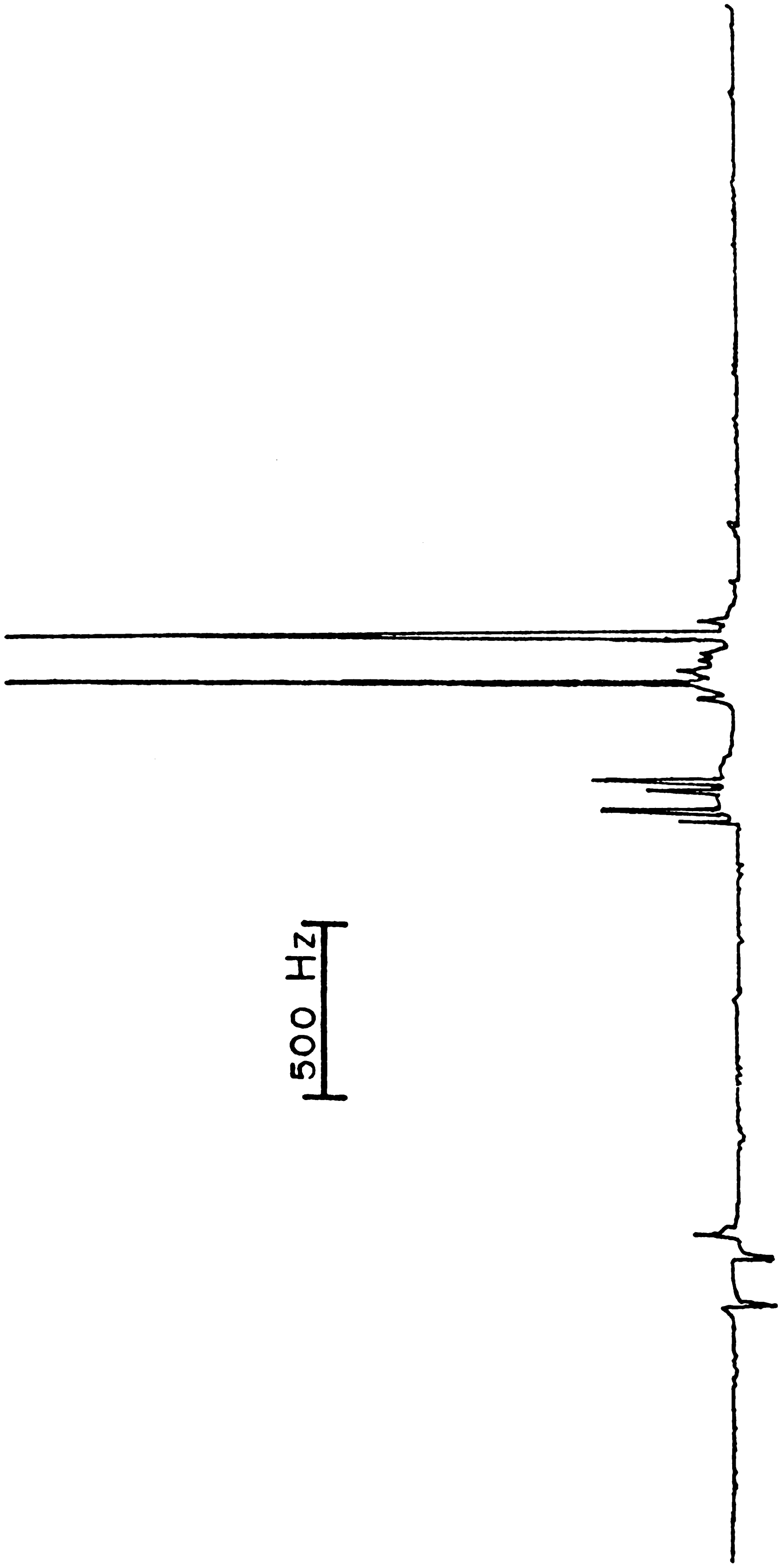
500 Hz

Table 2. ^{31}P and ^{19}F NMR Data

Compound	δ (ppm)[a]	J_{Rh-P} (Hz)
$Rh(PPh(CH_3)_2)_3BF_4$[b]	+5.9 d[c] -5.2 dd	135 84
$O{=}PPh(CH_3)_2$	-39.2	
$PPh(CH_3)_2$	+46.8	
$Rh(PPh(CH_3)_2)_3Cl_3$[d]	+5.5 -4.4	112 86
$Rh(PPh(CH_3)_2)_3BF_4$[e]	+152	
$NaBF_4$ in methanol	+154	

a) Parts per million for ^{31}P nmr were measured from 85% H_3PO_4, and for fluorine-19 nmr from $CFCl_3$.

b) Phosphorus-31 data

c) d = doublet, dd = doublet of doublets

d) Data for this complex were taken from reference 60.

e) Fluorine-19 data

The nmr data are consistent with the solution spectrum shown in Figure 11.

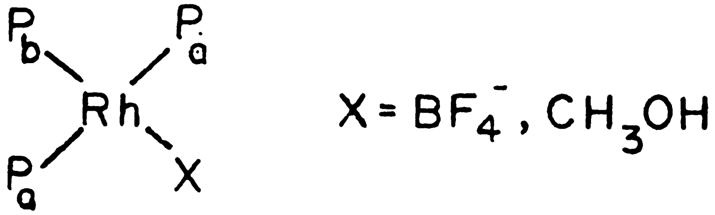

Figure 11. Solution structure of $Rh(PPh(CH_3)_2)_3BF_4$

Another source of the splitting of the signal for the unique phosphorus (P_b) in the ^{31}P nmr could be that two different RhL_3X^+ complexes exist in solution. The signals due to the phosphines (P_a) trans to each other in each of the complexes would have to be coincidental. The possibility of two complexes in solution seems unlikely, since the ratio of relative intensities in the phosphorus-31 spectrum for P_a and P_b is 2:1, and the line width of the signal assigned to P_a is narrow (1.5 Hz).

In tris phosphine rhodium complexes, the coupling constant, J_{Rh-P} has been shown to be always larger for phosphorus trans to each other than for phosphorus ligands cis to the other phosphorus atoms and trans to a halogen.[60,61]

The uv-visible spectrum of $Rh(PPh_3)_3BF_4$ is shown in Figure 12. The spectrum is dominated by a intense high energy band which consists of several peaks in the region of 250-275 nm. These peaks arise from transitions in triphenylphosphine.[62] The spectrum also exhibits two inflections at 316 and 363 nm on the steeply rising high energy band.

Figure 12. UV-Visible Spectrum of $Rh(PPh_3)_3BF_4$ in methanol

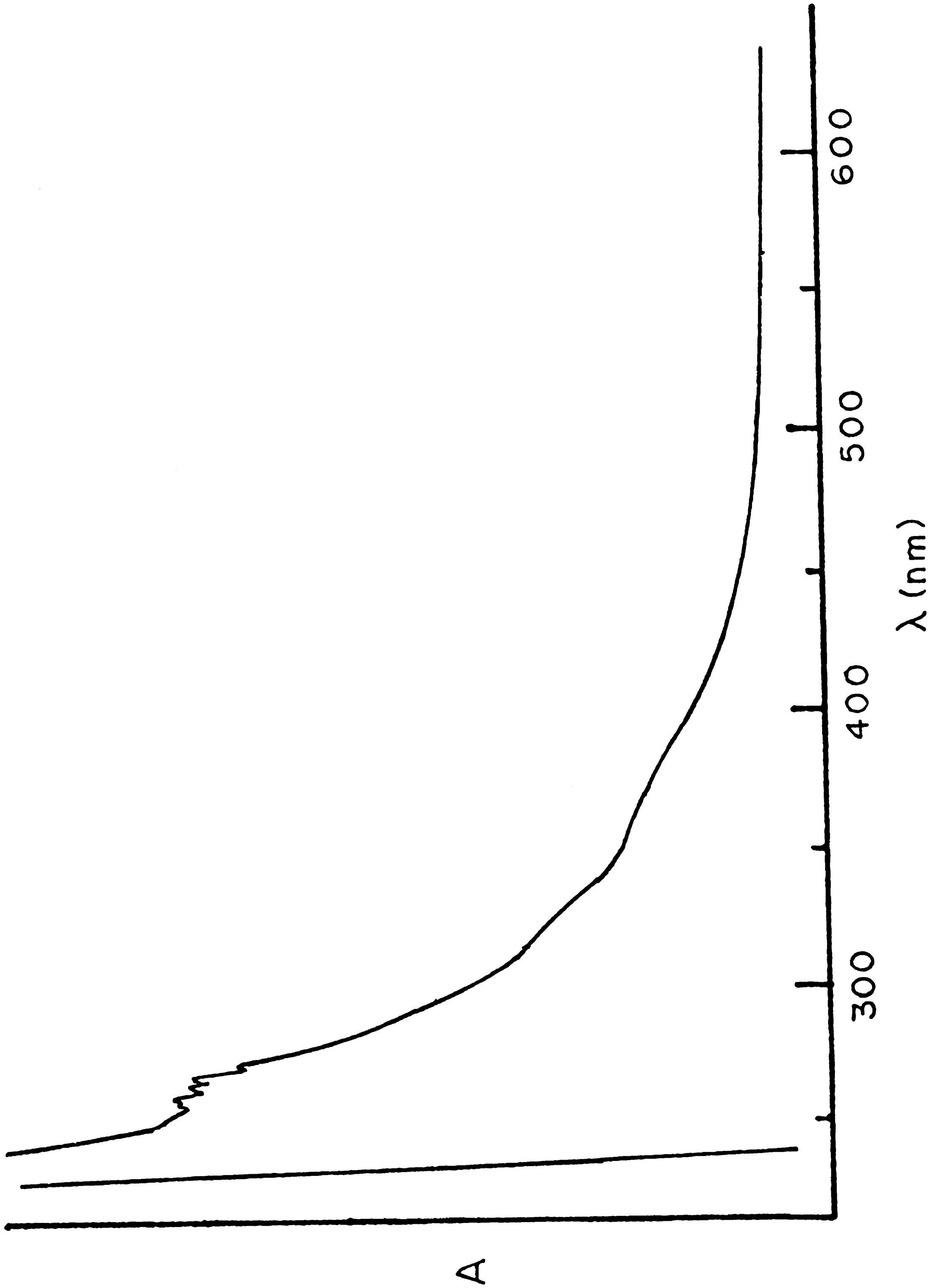
A
λ (nm)
300
400
500
600

B. Characterization of the Heterogeneous Catalyst

It was found that $Rh_2(CH_3COO)_{4-x}^{x+}$ could be introduced into the exchange sites of Na^+-hectorite by the treatment of the methanol-wet mineral with a methanol solution of $Rh_2(CH_3COO)_{4-x}^{x+}$ in the absence of air. The amount of the rhodium species exchanged onto the mineral could be controlled by varying the concentration of the rhodium solution (*cf*. Table 3).

Table 3. Rhodium Loading on Hectorite

Initial Concentration of $Rh_2(CH_3COO)_{4-x}^{x+}$	Number of Washes[a]	g of clay	wt% Rh
$8.0\text{x}10^{-3}\underline{M}$	3	0.5	1.51
$8.0\text{x}10^{-3}\underline{M}$	1	0.5	1.20
$2.0\text{x}10^{-3}\underline{M}$	1	0.5	0.75[b]

a) The methanol-wet mineral was washed with 10 ml of rhodium solution for 1-2 minutes, the solution filtered off and the mineral rinsed six times with methanol.

b) Average of four analyses ($\sigma = \pm 0.03$)

For the catalytic studies, one equivalent of native hectorite was slurried with 0.11 equivalents of the protonated rhodium species ($2.0\text{x}10^{-3}\underline{M}$) under oxygen-free conditions. The partially exchanged mineral had a rhodium content which corresponds to 12% of the CEC.

Upon treatment with the green-colored $Rh_2(CH_3COO)_{4-x}^{x+}$

solution, the white mineral immediately changes color to green. When the $2.0\times10^{-3}\underline{M}$ solution was used in the exchange reaction, most of the color in the solution was lost.

The infrared spectra of two rhodium exchanged hectorites are shown in Figure 13. Spectra A and B are shown for comparison. A is the spectrum of air-dried native hectorite, which has been treated with HSO_4^-. The clay was prepared as a self-supported film. After treatment with methanol, native hectorite exhibits a spectrum as shown in B. The spectrum of the emerald green mineral (*cf*. Figure 13C) exhibits two peaks at 1575 and 1453 cm^{-1} which are assigned to the asymmetric and symmetric stretches of the carboxylate group of the bidentate acetate ligands.[54,63]

The $Rh_2(CH_3COO)_{4-x}^{x+}$ ion on the mineral exhibits an intense band at 257 nm in the electronic spectrum. A similar band at 258 nm ($\varepsilon = 3.2\times10^3$) is observed in the solution spectrum. The bands in the visible region at 615 nm ($\varepsilon = 131$) and 427 nm ($\varepsilon = 131$) are not ovserved in the mineral bound species due to their low molar absorptivites and scattering effects of the mull sample. The infrared and electronic spectra indicate that the homogeneous cationic complex and the mineral bound species are similar.

An exchange reaction between $Rh_2(CH_3COO)_{4-x}^{x+}$ and biotite, attapulgite, talc, pyrophyllite, or kaolinite, minerals whose exhange capacity arises predominately from edge sites, did not lead to any observable binding of the ion.[64] Montmorillonite, a smectite whose negative charge on the silicate

Figure 13. Infrared Spectra of Various Hectorites; (a) Sodium(I)-Hectorite After Treatment with Sodium Bisulfate, (b) The Same Mineral After Washing with Methanol,

(c) $Rh_2(CH_3COO)_{4-x}{}^{x+}$-Hectorite, (d) $Rh(PPh_3)_x{}^{+}$-Hectorite

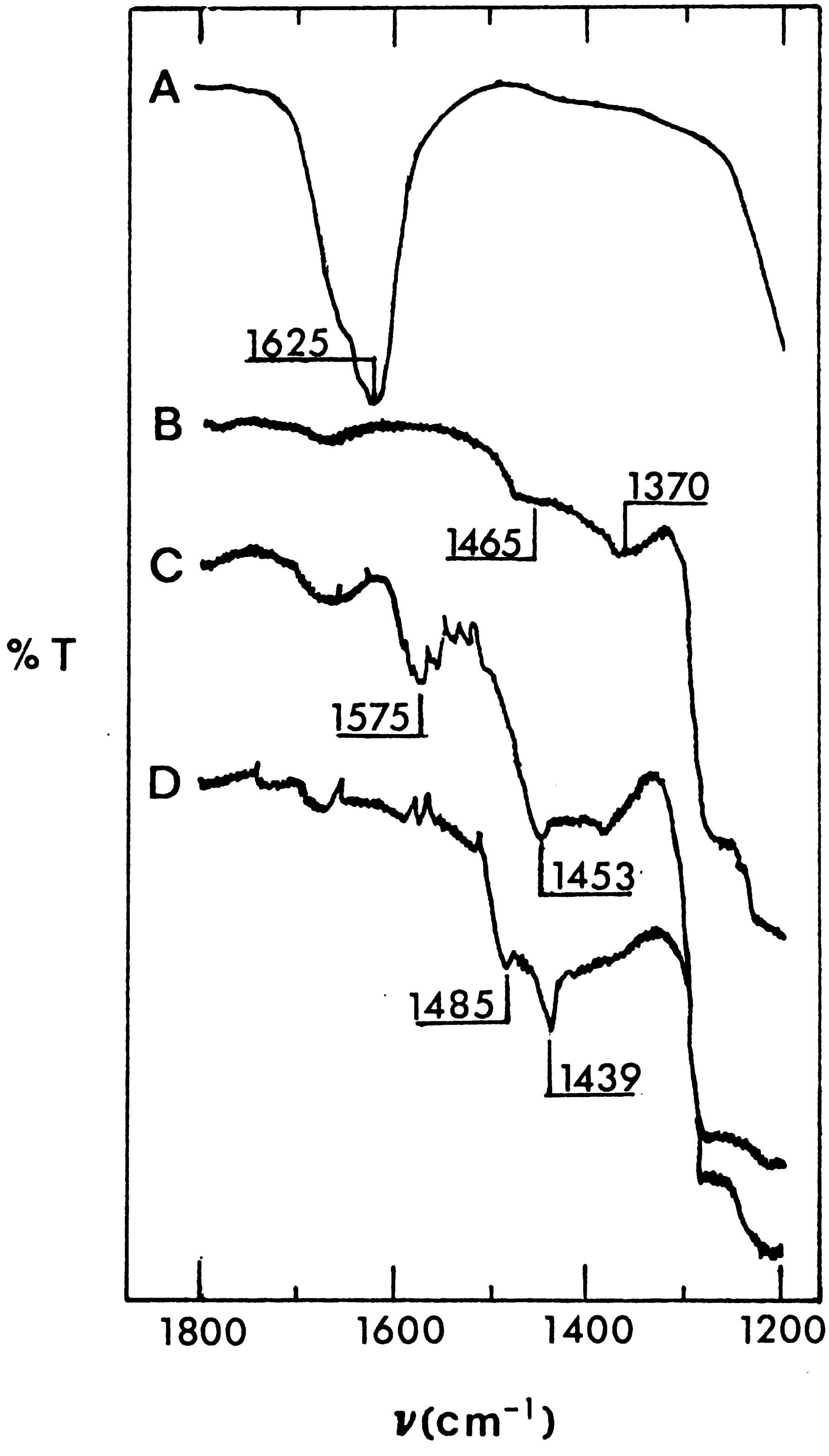
A
B
C
D
1625
1465
1370
1575
1453
1485
1439
% T
1800
1600
1400
1200
ν(cm^{-1})

sheets arises from isomorphous substitution of Mg^{2+} for Al^{3+} in the octahedral layer, readily binds $Rh_2(CH_3COO)_{4-x}{}^{x+}$. It is likely, therefore, that the complex is bound to the planar surfaces of the mineral, and not on the external edge sites.

Upon the addition of triphenylphosphine, the green colored mineral immediately changes color to a dark orange. A completely analogous reaction and color change occurs with the homogeneous catalyst (vide supra). The infrared spectrum, shown in Figure 13D, exhibits two peaks at 1485 and 1439 cm^{-1} which are assigned to in plane deformations of the phenyl rings bonded to phosphorus.[65] Both bands which were assigned to coordinated acetate in $Rh_2(CH_3COO)_{4-x}{}^{x+}$-hectorite disappear upon the addition of PPh_3.

The uv-visible spectrum for $Rh(PPh_3)_x{}^{+}$- hectorite is shown in Figure 14. This spectrum has several features which indicate again that the mineral bound species is similar to the homogeneous complex, $Rh(PPh_3)_3BF_4$. The spectrum is dominated by a high energy band which is poorly resovled into a series of peaks between 250-275 nm. Inflections are also observed at 315 and 367 nm on the high energy band. These same features are exhibited in the solution spectrum (cf. Figure 12).

Rhodium(II) benzoate, $Rh_2(C_6H_5COO)_4$, is protonated in methanol with HBF_4 in a manner similar to rhodium(II) acetate. The resulting $Rh_2(C_6H_5COO)_{4-x}{}^{x+}$ species is also readily exchanged onto the surfaces of hectorite. The product of the reaction between this mineral bound species and

Figure 14. UV-Visible Spectrum of $Rh(PPh_3)_x^+$-Hectorite

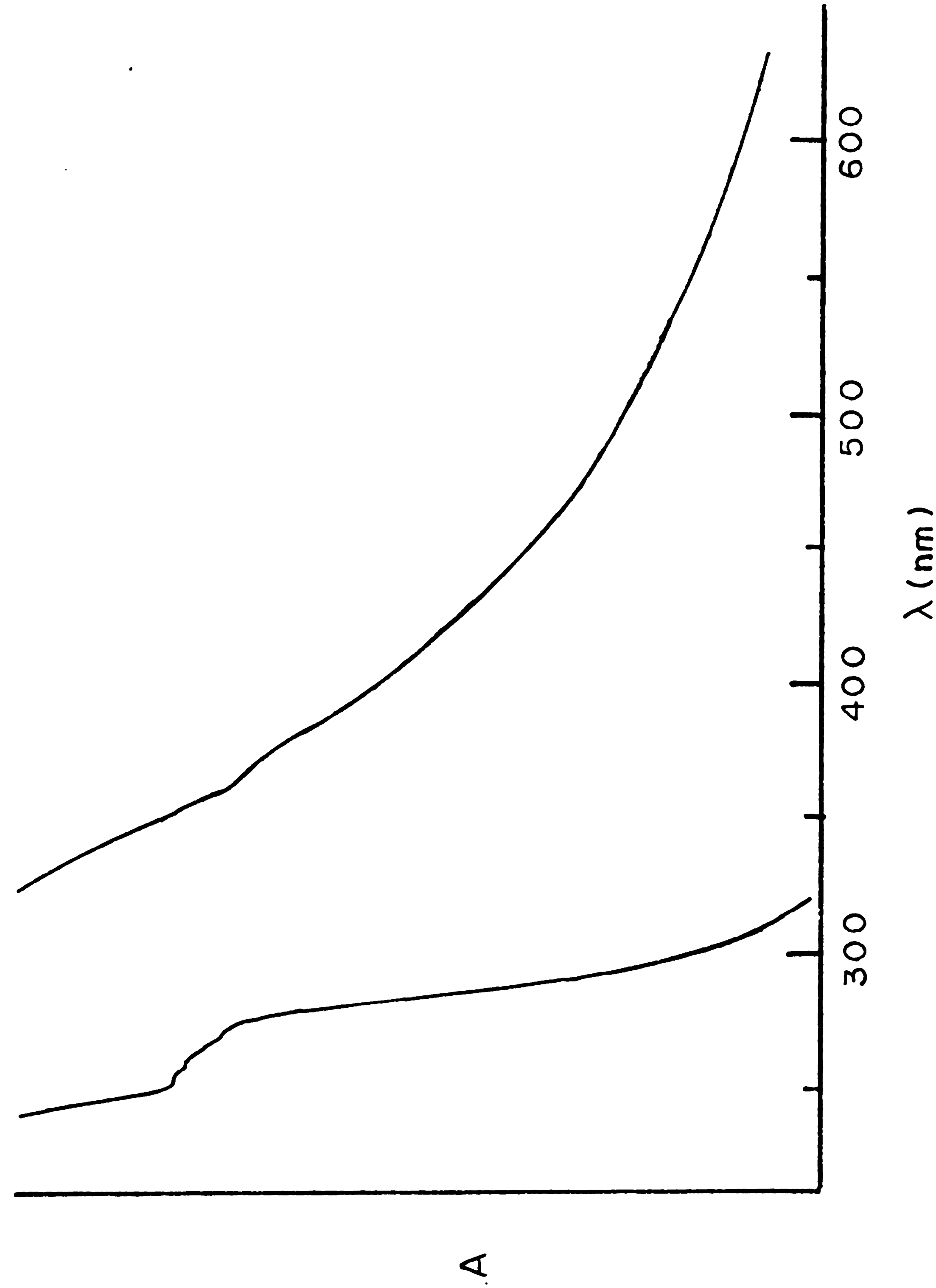
A
300
400
500
600
λ (nm)

triphenylphosphine is a dark orange species whose infrared spectrum contains the same peaks as $Rh(PPh_3)_x^+$-hectorite prepared from the related protonated rhodium acetate species. The fact that both the protonated acetate and benzoate complexes are catalyst precursors indicates that the catalytically active species does not contain an acetate ligand. These supported rhodium phosphine complexes are both catalysts for the hydrogenation of unsaturated hydrocarbons.

C. Hydrogenation Studies

$Rh(PPh_3)_x^+$-hectorite functions as an effective catalyst for the hydrogenation of alkenes and alkynes in methanol after treatment of the orange mineral with hydrogen. The complex on the mineral undergoes an oxidative addition of hydrogen to give a light yellow colored mineral, presumably $RhH_2(PPh_3)_x^+$-hectorite. An analogous reaction occurs in the preparation of the homogeneous catalyst.

Catalytic activity was found to be at a maximum for the mineral bound catalyst (wt% Rh = 0.76) when the PPh_3 concentration initially in the slurry was 4.6×10^{-3} M. This concentration corresponds to a PPh_3:Rh ratio of 9.5:1. The value of x in $Rh(PPh_3)_x^+$-hectorite is not likely to be greater than three as in the analogous homogeneous complex, $Rh(PPh_3)_3BF_4$. No catalytic reaction is observed with the supported catalyst when the initial phosphine concentration is less than 1.0×10^{-3} M (PPh_3:Rh = 2).

In order to understand better the reason for the large excess of PPh_3 needed for maximum catalytic activity, the adsorption of triphenylphosphine on Na^+-hectorite was studied. Various amounts of the phosphine were added to a methanol slurry of the mineral. After 5 minutes, an aliquot of the supernatant was removed. The absorbance of the supernatant at 260 nm was measured, and the amount of phosphine left in solution was calculated. The difference between the amount of phosphine initially added to the solution and the amount found in the supernatant is the quantity of PPh_3 adsorbed on the mineral. By plotting the moles of phosphine initially in solution versus the moles adsorbed, an adsorption curve of PPh_3 on native hectorite is obtained (cf. Figure 15). This figure shows that at low concentrations of PPh_3, little phosphine is adsorbed, so the amount of phosphine which reaches the rhodium(II) acetate complex will be small, probably less than 2 moles per rhodium atom. With the homogeneous catalyst, a PPh_3:Rh ratio of two gave the maximum catalytic activity.[3] As the concentration of the phosphine is increased the fraction of total phosphine adsorbed increases abruptly, which indicates that the phosphine has penetrated the intercrystalline space. At the higher concentrations of PPh_3, the phosphine penetrates between the layers to react with the exchanged rhodium complex. Another function of PPh_3 in the intralamellar space is that this large bulky molecule might act as a molecular prop, so that the reactants might have an easier access to the catalytic site.

Initial rates over the first 8-10% of the reaction for

Figure 15. Adsorption Curve of Triphenylphosphine on Na^+-Hectorite

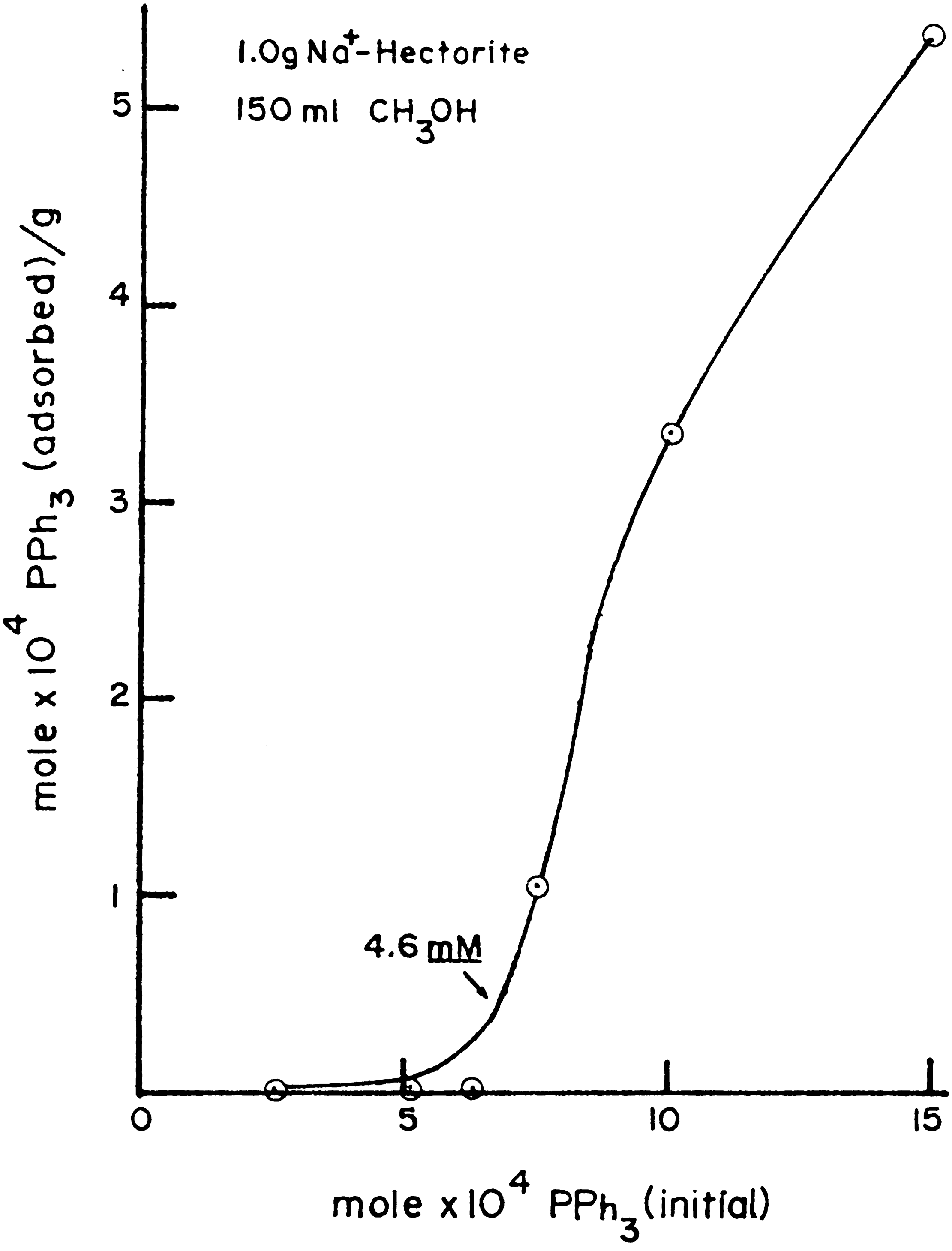
1.0g Na+-Hectorite
150 ml CH3OH
4.6 mM
mole x 10^4 PPh3 (adsorbed)/g
1
2
3
4
5
0
5
10
15
mole x 10^4 PPh3 (initial)

for the reduction of alkenes and alkynes at 25°C are presented in Tables 4 and 5. In both tables, turnover numbers (ml of H_2/min/mmole of Rh) are used to report the initial rates of hydrogenation. For comparison, the rates of hydrogenation of the substrates relative to 1-hexene are also given in these tables. The relative rates for the homogeneous catalyst are calculated from the data reported by Wilkinson and co-workers.[3]

Terminal olefins are reduced with a linear uptake of H_2 to the corresponding alkane, with the exception of 3,3-dimethyl-1-butene which does not undergo hydrogenation. Products of these reductions were identified by gas chromatography. For the hydrogenation of 1-heptene, some 2-heptene was found in the product mixture. Some isomerization most likely occured in the hydrogenation of 1-hexene, but 2-hexene was not separated from the reaction mixture by gas chromatography. The retention times for 2-hexene and 1-hexene were found to be nearly the same on the SE-30 column. Representative graphs of the hydrogenation rates of unsaturated hydrocarbons are shown in Figures 16-19.

Terminal olefins with other functional groups within the molecule, eg., -OR and -OH, are reduced with a non-linear H_2 uptake. The non-linear uptake of H_2 indicates that the reduction of these olefins is a more complicated process than the reduction of terminal olefins. The reaction products were not identified for the hydrogenation of these olefins. Several possibilites are plausible as to why the reduction

Table 4. Hydrogenation Rates[a] of Alkenes in the Presence of Mineral Supported and Homogeneous Rh(I)-PPh_3 Catalysts

Substrate	Mineral Supported Catalyst ml H_2/min/mmole Rh	Mineral Supported Catalyst Relative Rate	Homogeneous Catalyst Relative Rate[b]
1-hexene	10.5	1.0	1.0[c]
1-heptene	7.3	0.7	-
2-hexene (cis & trans)	N.R.	0.0	0.3
3,3-dimethyl-1-butene	N.R.	0.0	-
cyclohexene	N.R.	0.0	-
1,5-hexadiene	98.5	9.4	3.6
allyl phenyl ether	15.0	1.4	1.4
allyl alcohol	17.9	1.7	-

a) Conditions

$[PPh_3] = 4.6$ m$\underline{M}$

wt% Rh = 0.75 → 1.47×10^{-5} mole Rh/0.2g sample

[olefin] = 1.0$\underline{M}$

total volume = 30 ml

Temperature = 25°C

Solvent = Methanol with 0.2% H_2O

P_{H_2} = 600 torr

Table 4 (cont'd)

b) Relative rates for homogeneous catalyst calculated from data found in reference 3.

c) Turnover number found to be 140 ml H_2/min/mmole Rh in this study.

Figure 16. Plot of the Hydrogenation Rate of 1-Hexene

Conditions:

0.2g of $Rh_2(CH_3COO)_{4-x}{}^{x+}$-hectorite (0.76% Rh)
2.8 ml of 0.05$\underline{M}$ PPh_3
3.75 ml of 1-hexene
total volume = 30 ml

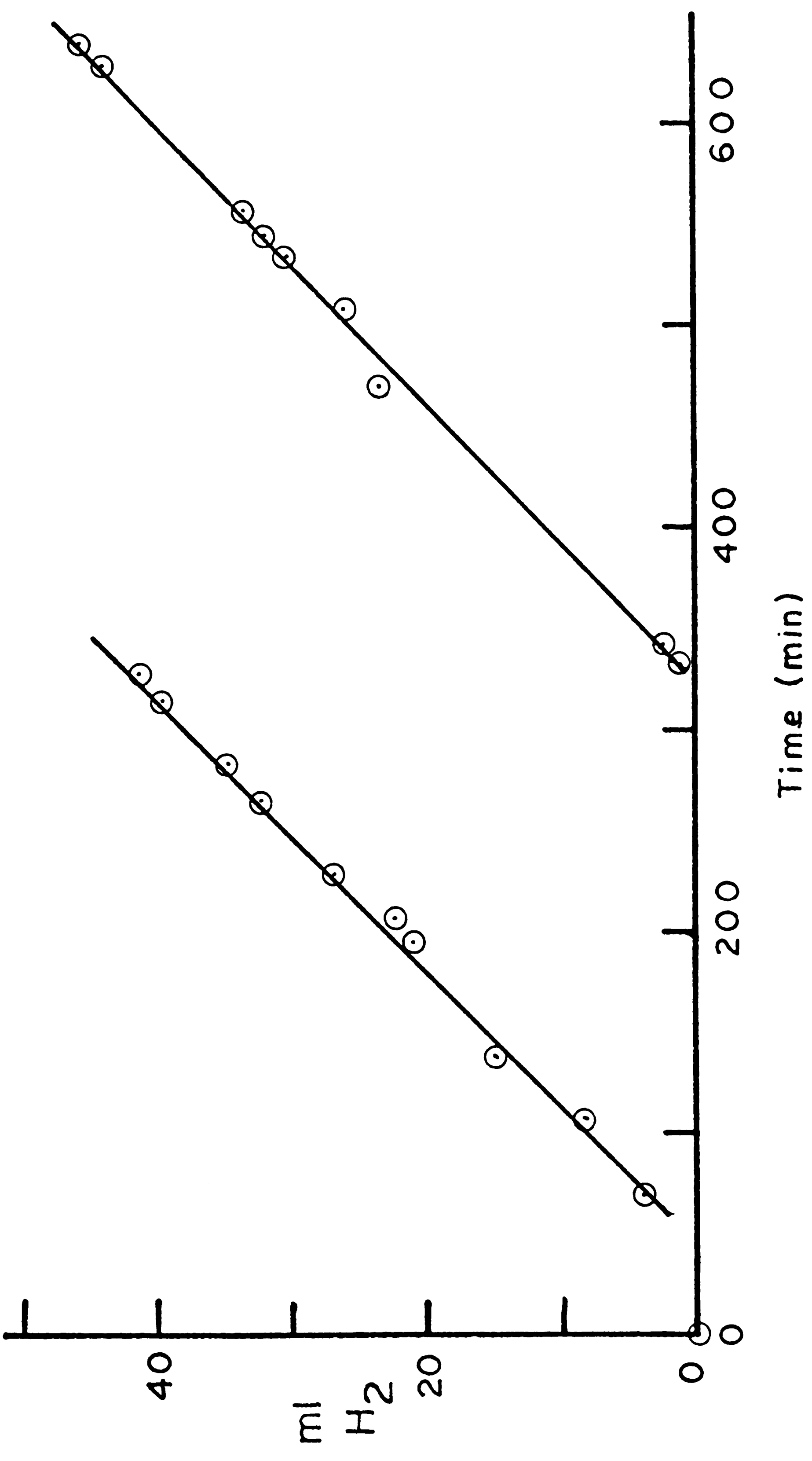
ml
H_2
0
20
40
0
200
400
600
Time (min)

of these substituted olefins occurs with a non-linear H_2 uptake. The substrate could irreversibly bind to the metal ion via the functional group, which would prevent further coordination of the olefin and hydrogen; or a side reaction could occur concurrently with the hydrogenation reaction. Polymerization and hydrogenolysis are examples of the type of reaction which modifies the substrate, therefore, the reactivity of the olefin to the catalyst would change. Rylander has reported that the allylic group is especially susceptible to hydrogenolysis.[66a] Catalytic hydrogenolysis is defined as "the cleavage of a molecule into fragments by hydrogen in the presence of a catalyst."[66a] Three possible reactions can occur in the hydrogenolysis of the allylic function: the splitting out of water from allylic alcohol with or without the subsequent reduction of the olefin, the reduction of the allylic group, and the formation of a ketone of aldehyde by a migration of the double bond.[66b] If both an aldehyde or a ketone were formed by the migration of the double bond, and the allylic function were reduced, a non-linear uptake of hydrogen would be observed.

Internal olefins are not reduced by the mineral supported catalyst to any observable extent. Internal olefins are hydrogenated at a much slower rate than terminal olefins with a homogeneous catalyst.[3] Internal olefins are reported to have a smaller association constant for coordination to the metal ion than terminal olefins,[67] which could account for the reduced activity in solution. Steric factors

Figure 17. Plot of the Hydrogenation Rate of Allyl Alcohol

Conditions:

0.2g of $Rh_2(CH_3COO)_{4-x}^{x+}$-hectorite (0.76% Rh)
2.8 ml of 0.05$\underline{M}$ PPh_3
2.0 ml of allyl alcohol
total volume = 30 ml

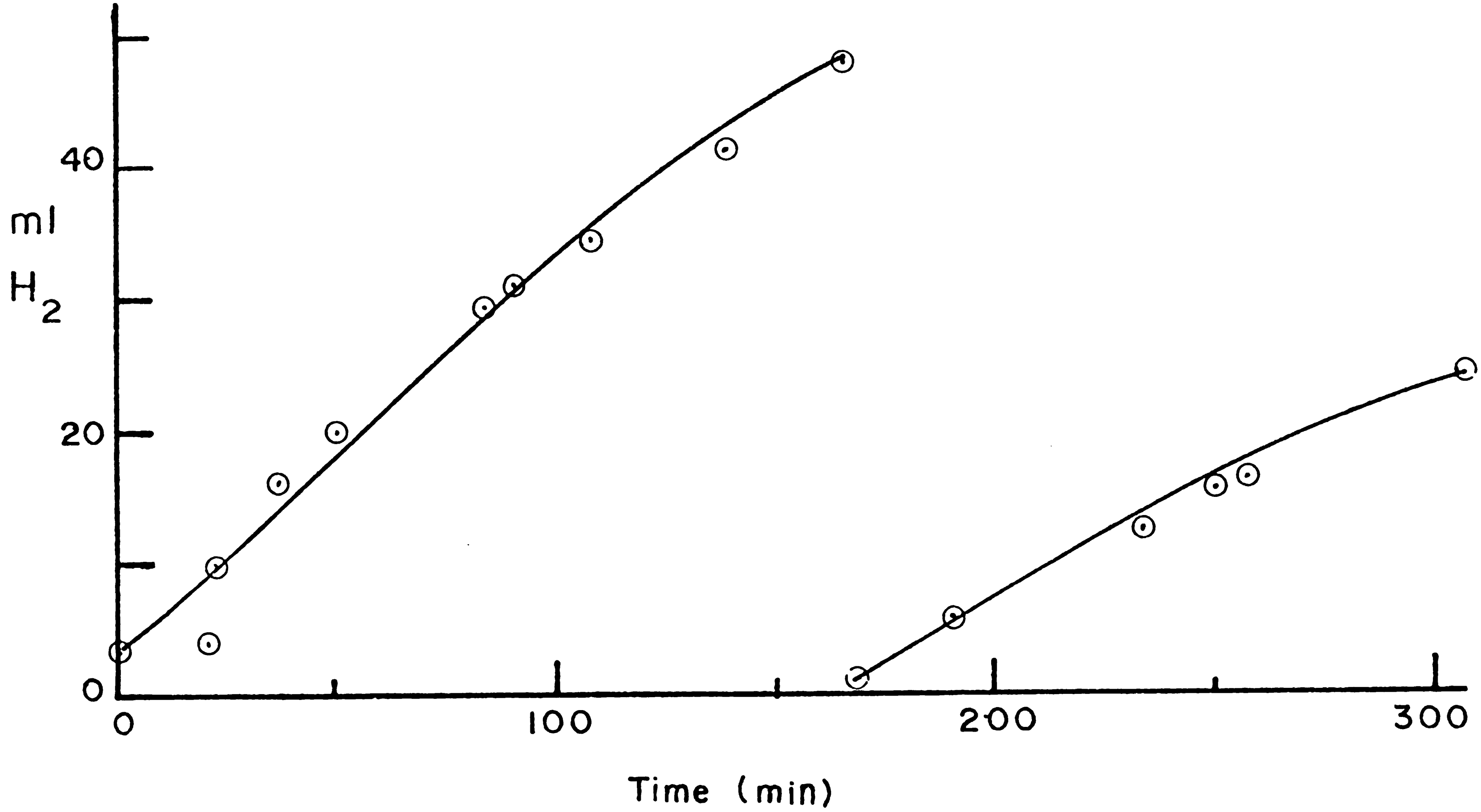
ml
H_2
0
20
40
0
100
200
300
Time (min)

are generally considered to effect the coordination ability of an olefin to bind to a metal. With the mineral supported catalyst, the olefin must react with the catalyst in a sterically restrictive environment which might magnify the steric effects.

The trends in the relative rates of reaction for the supported and the homogeneous catalysts parallel each other, which means that similar species catalyze the reactions on the surface and in solution. The mineral environment, however, exerts an inhibitive effect on the actual rate of hydrogenation. The homogeneous catalyst reduces olefins at a rate an order of magnitude faster than the supported catalyst. Friedlander[68] reported that olefins do not penetrate into the intralamellar space of smectites. This lack of penetration of the olefin into the intracrystalline space would lead to a concentration gradient between solution and the catalytic site. The concentration of the olefin at the catalytic site in the mineral would be less than 1.0M, the initial olefin concentration in solution.

Terminal alkynes as well as internal alkynes are reduced with a linear H_2 uptake with the supported catalyst (cf. Figure 18). The hydrogenation reactions of these substrates were followed by gas chromatography. The chromatographic data show that terminal alkynes are hydrogenated in a stepwise manner, first with reduction to the alkene, then to the alkane. A new molecule of alkyne will displace the alkene from the coordination sphere of the metal as long as

Table 5. Hydrogenation Rates[a] of Alkynes in the Presence of Mineral Supported and Homogeneous Rh(I)-PPh_3 Catalysts

	Mineral Supported Catalyst		Homogeneous Catalyst
	ml H_2/min/mmole Rh	Relative Rate	Relative Rate[b]
1-hexyne	530	50	3.1
2-hexyne	530	50	-
1-octyne	680	65	-
phenyl acetylene	130	12	-
3-butyn-1-ol	480	46	-
propargyl alcohol	315	30	1.6
propargyl chloride	32	3.0	-
2-methyl-3-butyn-2-ol	600	57	4.1[c]

a) Conditions are the same as those presented in Table 4.

b) Relative rates for homogeneous catalyst calculated from data found in reference 3.

c) Turnover number found to be 280 ml H_2/min/mmole Rh in this study.

Figure 18. Plot of the Hydrogenation Rate of 1-Hexyne

Coditions:

0.2g of $Rh_2(CH_3COO)_{4-x}{}^{x+}$-hectorite (0.76% Rh)
2.8 ml of 0.05$\underline{M}$ PPh_3
3.4 ml of 1-hexyne
total volume = 30 ml

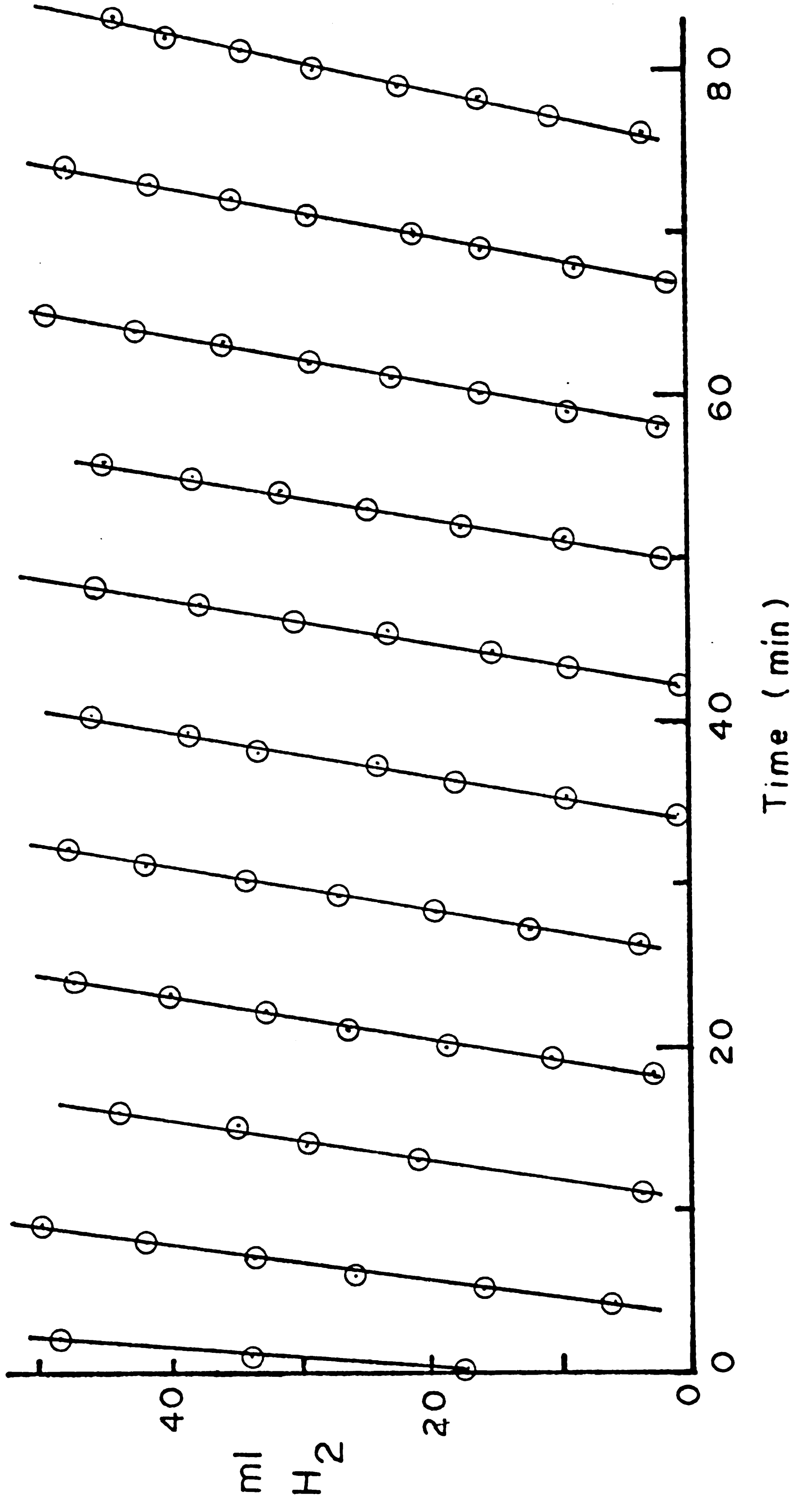
ml
H_2
40
20
0
0
20
40
60
80
Time (min)

the alkyne is present in a large excess. As the concentration of the alkyne decreases, the hydrogenation of the alkene becomes more important. In the reduction of internal alkynes, no hydrogenation of the alkene was observed. Internal olefins were not reduced with this mineral supported catalyst (*vide supra*). Recently, a similar observation, 2-hexyne being selectively reduced to *cis*-2-hexene has been reported.[69] The catalyst used in that study was a cationic homogeneous complex, $Rh(NBD)(PPh_3)_2^+$. After the alkyne was totally reduced to the alkene, the resulting olefin undergoes hydrogenation and isomerization.

Substituted alkynes as is the case with substituted olefins undergo hydrogenation with a non-linear H_2 uptake (*cf*. Figure 19). Again it seems likely that some side reaction is occurring at the same time as the hydrogenation reaction. Alkynes with an oxygen adjacent to the triple bond are known to undergo hydrogenolysis to various extents.[66c] Water or an alcohol would be split from the alkyne to yield a simple alkyne. The substituted alkynes might also undergo dimerization or polymerization. $RhCl(PPh_3)_3$ is known to be an active catalyst for the polymerization of the substituted alkynes studied in this project.[70] Propargyl chloride poisons the catalyst by undergoing an oxidative addition reaction with the metal complex.[70]

The relative rates of hydrogenation for the supported and the homogeneous catalysts also follow parallel trends as is the case with the olefins. Similar catalytic species are

Figure 19. Plot of the Hydrogenation Rate of Propargyl Alcohol

Conditions:

0.2g of $Rh_2(CH_3COO)_{4-x}{}^{x+}$-hectorite (0.76% Rh)
2.8 ml of 0.05$\underline{M}$ PPh_3
1.75 ml of propargyl alcohol
total volume = 30 ml

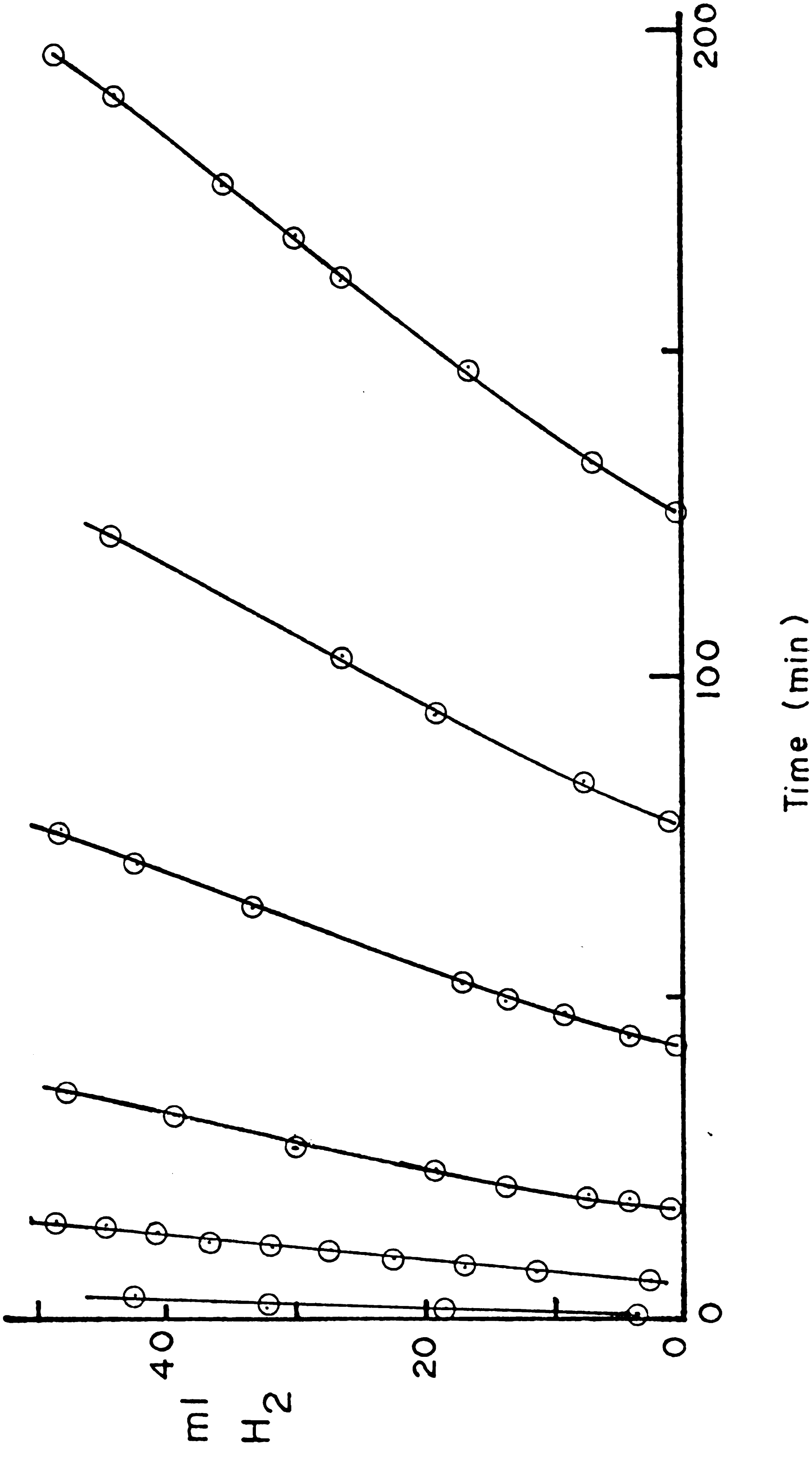
Time (min)
0
100
200
ml H$_2$
0
20
40

involved in both the heterogeneous and homogeneous systems. The rate of reduction of alkynes is faster than that of olefins. The increased rate of hydrogenation means that the substrate is more readily accessible to the catalytic site than in the case of the olefins.

The turnover numbers were found to be dependent on the amount of rhodium complex exchanged onto the mineral. If only a fraction of the complex is involved in the catalytic reaction, the turnover number is not an adequate representation of the true activity of the complex. The data presented in Table 6 illustrates how the turnover number changes with the rhodium content of the mineral.

Table 6. Effect of Rhodium Loading on the Turnover Number

wt% Rh	Rate[a] (ml/min)	Turnover Number (ml/min/mmole)
1.51	0.14	4.2
1.20	0.15	6.5
0.76	0.14	9.5

a) Rates are for the hydrogenation of 1-hexene. Triphenylphosphine was added so that the initial concentration corresponded to a PPh_3:Rh ratio of nine.

The reaction occurs within the first 10-20 Å of the intralamellar space of the mineral. At the higher loadings of rhodium, metal atoms are further into the crystal, and therefore, not accessible to the reactants.

IV. CONCLUSIONS

This investigation has shown that a homogeneous hydrogenation catalyst can be supported on hectorite, a naturally occurring crystalline silicate mineral, without loss of activity. Infrared and uv-visible spectra show the mineral bound species is chemically similar to the homogeneous complex. The selectivity of the complex, though, is affected by the mineral environment as shown by the study of a variety of alkenes and alkynes. Terminal olefins are hydrogenated at a rate slower than with the homogeneous catalyst, and internal olefins are not reduced to any appreciable extent. The usefulness of the mineral supported catalyst is demonstrated by the hydrogenation of 2-hexyne, which is reduced to 2-hexene only. No hexane was observed in the product mixture. Terminal alkynes are reduced by the mineral supported catalyst at an initial rate comparable to the soluble catalyst.

The catalyst precursor, $Rh_2(CH_3COO)_{4-x}{}^{x+}$, was found to contain coordinated acetate ligands, but from the pmr data, the exact nature of the complex could not be elucidated. Triphenylphosphine was found to act as the reducing agent in the formation of $Rh(PPh_3)_3BF_4$ from $Rh_2(CH_3COO)_{4-x}{}^{x+}$.

BIBLIOGRAPHY

BIBLIOGRAPHY

1. H. Heinemann, Chem. Tech., 286(1971).

2. B. R. James, "Catalytic Hydrogenation," John Wiley & Sons, Inc. New York, N. Y., 1973.

3. P. Legzdins, R. W. Mitchell, G. L. Rempel, J. D. Ruddick, and G. Wilkinson, J. Chem. Soc.(A), 3322(1970).

4. R. E. Grim, "Clay Mineralogy," 2nd ed., McGraw-Hill Book Co., New York, N. Y., 1968 pp. 1-3.

5. H. van Olphen, "An Introduction to Clay Colloid Chemistry," John Wiley & Sons, Inc., New York, N. Y., 1963 pp. 68-69.

6. W. T. Granquist, "Chemistry of Clays and Clay Minerals," Editor, J. J. Fripiat, in press.

7. D. B. Fenn, M. M. Mortland, and T. J. Pinnavaia, Clays and Clay Minerals, **21** 315(1973).

8. Sharmaine S. Cady, Ph.D. Dissertation, Department of Chemistry, Michigan State University, 1976.

9. T. J. Pinnavaia, and P. K. Welty, J. Am. Chem. Soc., **97** 3819(1975); T. J. Pinnavaia, P. K. Welty, and J. F. Hoffman, Proc. Int. Clay Conference, Mexico City, 373(1975).

10. I. I. Chernyaev, E. V. Shenderetskaya, L. A. Nozarova, and A. S. Antsyshkina, Abstracts of Papers Presented at 7th International Conference on Coordination Chemistry, Stockholm, 1962.

11. M. A. Porai-Koshito, and A. S. Antsyshkina, Dakl. Akad. Nauk. SSSR, **46** 1102(1962).

12. S. A. Johnson, H. R. Hunt, and H. M. Neumann, Inorg. Chem., **2** 960(1963).

13. F. A. Cotton, and J. G. Norman, Jr., J. Am. Chem. Soc., **94** 5697(1972).

14. J. L. Bear, J. Kitchens, and M. R. Willcott, III, *J. Inorg. Nucl. Chem.*, **33** 3479(1971).

15. B. C. Hui, and G. L. Rempel, *Chem. Comm.*, 1195(1970).

16. B. C. Y. Hui, W. K. Teo, and G. L. Rempel, *Inorg. Chem.*, **12** 757(1973).

17. F. Maspero, and H. Taube, *J. Am. Chem. Soc.*, **90** 7361(1968).

18. J. J. Ziolkowski, and H. Taube, *Bull. Acad. Pol. Sci., Ser. Sci. Chim.*, **21** 113(1973).

19. J. J. Ziolkowski, *ibid.*, 119.

20. V. I. Belova, and Z. S. Dergacheva, *Russ. J. Inorg. Chem.*, **16** 1626(1971).

21. C. R. Wilson, And H. Taube, *Inorg. Chem.*, **14** 405(1975).

22. P. Legzdins, G. L. Rempel, and G. Wilkinson, *Chem. Comm.*, 825(1969).

23. C. R. Wilson, and H. Taube, *Inorg. Chem.*, **14** 2276(1975).

24. J. J. Ziolkowski, *Bull. Acad. Pol. Sci., Ser. Sci. Chim.*, **21** 125(1973).

25. L. Dubicki, and R. L. Martin, *Inorg. Chem.*, **9** 673(1970).

26. R. W. Mitchell, J. D. Ruddick, and G. Wilkinson, *J. Chem. Soc.(A)*, 3224(1971).

27. R. Z. Moravec, W. T. Schelling, and C. F. Oldershaw, British Patent 511,556(1939); *Chem. Abstr.*, **34** 7102(1940).

28. R. Z. Moravec, W. T. Schelling, and C. F. Oldershaw, Canadian Patent 396,994(1941); *Chem. Abstr.*, **35** 6103(1941).

29. G. J. K. Acres, G. C. Bond, B. J. Copper, and J. A. Dawson, *J. Catalysis*, **6** 139(1966).

30. P. R. Rony, *J. Catalysis*, **14** 142(1969).

31. P. R. Rony, and J. F. Roth, *J. Molec. Catalysis*, **1** 13(1975/76).

32. J. Manassan, *Platinum Metal Rev.*, **15** 142(1971).

33. Z. M. Michalska, and D. E. Webster, *Chem. Tech.*, 117 (1975); *Platinum Metal Rev.*, **18** 65(1974).

34. C. U. Pittman, Jr., and G. O. Evans, *Chem. Tech.*, 560(1973).

35. R. H. Grubbs, and L. C. Kroll, *J. Am. Chem. Soc.*, **93** 3062(1971).

36. R. H. Grubbs, L. C. Kroll, and E. M. Sweet, *J. Macromol. Sci.*, **A7** 1047(1973).

37. J. P. Collman, L. S. Hegedus, M. P. Cooke, J. R. Norton, G. Dolcetti, and D. N. Marquardt, *J. Am. Chem. Soc.*, **94** 1789(1972).

38. R. H. Grubbs, C. Gibbons, L. C. Kroll, W. D. Bonds, Jr., and C. H. Brubaker, Jr., *J. Am. Chem. Soc.*, **95** 2373 (1973).

39. W. Dumont, J. C. Poulin, T. P. Dang, and H. B. Kagan, *J. Am. Chem. Soc.*, **95** 8295(1973).

40. H. B. Kagan, and T. P. Dang, *J. Am. Chem. Soc.*, **94** 6429(1972).

41. H. Bruner, J. C. Bailar, Jr., *Inorg. Chem.*, **12** 1465 (1973).

42. D. R. Fahey, *J. Org. Chem.*, **38** 80(1973); *J. Org. Chem.*, **38** 3343(1973).

43. C. U. Pittman, Jr., L. R. Smith, and R. M. Hanes, *J. Am. Chem. Soc.*, **97** 1742(1975).

44. C. U. Pittman, Jr., and L. R. Smith, *J. Am. Chem. Soc.*, **97** 1749(1975).

45. C. U. Pittman, Jr., S. E. Jacobson, and H. Hiramoto, *J. Am. Chem. Soc.*, **97** 4774(1975).

46. S. E. Jacobson, C. U. Pittman, *Chem. Comm.*, 187(1975); S. Jacobson, W. Clements, H. Hiramoto, C. U. Pittman, Jr., *J. Molec. Catalysis*, **1** 73(1975/76).

47. K. G. Allum, R. D. Hancock, I. V. Howell, R. C. Pitkethly, and P, J. Robinson, *J. Organomet. Chem.*, **87** 189(1975).

48. K. G. Allum, R. D. Hancock, I. V. Howell, R. C. Pitkethly, and P. J. Robinson, *J. Organomet. Chem.*, **87** 203(1975); and references therein.

49. K. G. Allum, R. D. Hancock, I. V. Howell, T. E. Lester, S. McKenzie, R. C. Pitkethly, and P. J. Robinson, *J. Organomet. Chem.*, **107** 393(1976).

50. L. J. Boucher, A. A. Oswald, and L. L. Murrell, Preprint of paper presented before the Div. of Pet. Chem., A.C. S., Los Angeles, 1974.

51. E. Bayer, and V. Schurig, *Angew. Chem. Int. Ed.*, **14** 493(1975); *Chem. Tech.*, 212(1976).

52. G. W. Parshall, *J. Am. Chem. Soc.*, **94** 8716(1972).

53. G. L. Rempel, P. Legzdins, H. Smith, and G. Wilkinson, *Inorg. Syntheses*, **13** 90(1972).

54. T. A. Mal'kova, V. M. Shafranskii, *Zh. Neorg. Khim.*, **19** 2501(1974).

55. Reported value of CEC on assay received on centrifuged and spray-dried hectorite Bl-26 from Baroid, Division of NL Industries.

56. Dr. Murray B. McBride, Michigan State University, private communication.

57. $P(CH_3)Ph_2$ was prepared by literature methods. (B.P. = 190-195°C at 50 torr); M. A. Mathur, W. H. Myers, H. H. Sisler, and G. E. Ryschkewitsch. *Inorg. Syntheses*, **15** 129(1974).

58. D. D. Traficante, J. A. Sims, M. Mulcahy, *J. Magn. Res.*, **15** 484(1974).

59. Standard NMR Spectrum No. 10261, Sadtler Research Laboratories, Philadelphia, PA.

60. S. O. Grim, and R. A. Ference, *Inorg. Chim. Acta*, **4** 277(1970).

61. C. A. Tolman, P. Z. Meakin, D. L. Lindner, and J. P. Jesson, *J. Am. Chem. Soc.*, **96** 2762(1974).

62. H. Schindlbauer, *Monat. fur Chem.*, **94** 100(1963).

63. Y. Y. Kharitonov, G. Y. Mazo, and N. A. Knyazeva, *Zh. Neorg. Khim.*, **15** 1440(1970).

64. Philip K. Welty, Ph.D. Dissertation, Department of Chemistry, Michigan State University, 1974.

65. H. G. Horn, and K. Sommer, *Spectrochim. Acta A*, **27** 1049(1971).

66. P. N. Rylander, "Catalytic Hydrogenation over Platinum Metals," Academic Press, New York, N. Y., 1967, a) p. 433, b) p. 439, c) p. 75.

67. M. Herberbold, "Metal π-Complexes," Vol. II, Part 2, Elsevier, Amsterdam, 1974. Chap. VII and references therein.

68. H. Z. Friedlander, A.C. S., Div. Polymer Chem., Preprints **4** 300(1963); *Chem. Abstr.*, **63** 4393g(1965).

69. R. R. Schrock, and J. A. Osborn, *J. Am. Chem. Soc.*, **98** 2143(1976).

70. H. Singer, and G. Wilkinson, *J. Chem. Soc.(A)*, 849(1968).

MICHIGAN STATE UNIVERSITY LIBRARIES
3 1293 03085 4008